Anna Karner, BSc BSc

Positron Annihilation Lifetime Spectroscopy of cellulose materials during moisture intake

MASTER THESIS

to achieve the university degree of

Diplom-Ingenieurin

Master's degree programme

Technical Physics

submitted to

Graz University of Technology

Supervisor

Assoc.Prof. Dr.rer.nat. Wolfgang Sprengel

Institute of Materials Physics

Co-Supervisor

Dipl.-Ing. Laura Resch, BSc

Graz, June 2020

EIDESSTATTLICHE ERKLÄRUNG

AFFIDAVIT

Ich erkläre an Eides statt, dass ich die vorliegende Arbeit selbstständig verfasst, andere als die angegebenen Quellen/Hilfsmittel nicht benutzt, und die den benutzten Quellen wörtlich und inhaltlich entnommenen Stellen als solche kenntlich gemacht habe. Das in TUGRAZonline hochgeladene Textdokument ist mit der vorliegenden Masterarbeit identisch.

I declare that I have authored this thesis independently, that I have not used other than the declared sources/resources, and that I have explicitly indicated all material which has been quoted either literally or by content from the sources used. The text document uploaded to TUGRAZonline is identical to the present master's thesis.

Datum / Date	Unterschrift / Signature

ACKNOWLEDGMENTS

I would like to express my gratitude first to all members of the Institute of Material Physics, especially the head of the Institute, Professor Roland Würschum, for including me in the team in such a kind way and allowing me to gain stimulating insights into the interesting fields of materials physics.

My deep gratitude goes to my supervisor, Professor Wolfgang Sprengel, for his guidance, sharing his knowledge with me and his support during the whole time of the thesis.

Also, I have to say a big thank you to Laura Resch, who patiently explained to me all my questions on positron and positronium physics, always had useful suggestions, helped me with all my experiments and analysis and not just improved my work in laboratory but also made it a lot more fun.

At this point, I would like to say thank you to Professor Robert Schennach and Professor Karin Zojer from the Institute of Solid State Physics for sharing their expertise on paper physics and chemistry with me. As well, I have to express my gratitude to the CD-Labor “für Stofftransport durch Papier” for providing the paper samples.

At this point, I want to thank my family for their support and help in every situation of my life.

Last but not least, I also want to say thank you to my friends and colleagues who made the last five years in Graz an exciting and unforgettable period in my life.

ABSTRACT

In the present thesis cellulose and paper materials during moisture intake and the corresponding pore size change were investigated. Due to their product performance and possible applications, especially for materials with cellulose content, knowledge about the processes occurring during moisture intake are of great relevance. The experimental method applied was Positron Annihilation Lifetime Spectroscopy (PALS), which is a non-destructive tool for probing open volume defects and porosity of materials. Complimentary to PALS, other methods like contact angle measurements and water content detection were used to gain more insights into the investigated cellulose material samples.

Within this work, the positron lifetime in three different cellulose materials (pure cellulose, fine paper and Kraft sack paper) was measured during a cycle of moistening and drying. The idea is to monitor the pore size during this process via PALS. The PALS data was fitted and analysed using the software PALSfit.

These measurements offered some very interesting results; for example, that the mean positron lifetime – respectively the pore size – increases, as expected, with the water content in the materials, however, the increase of the mean positron lifetime lasts more than ten times as long as the increase of the water content. Worth mentioning is also that the process of moistening and drying the samples seems to be reversible; this means that the mean positron lifetime of the samples before moistening and after drying are about the same amount.

Another interesting finding is, that cellulose and Kraft sack paper samples show two plateaus when monitoring the mean positron lifetime in dependence of time. This suggests that there are two processes on different time scales. The results also show that the material with the highest water intake – which is cellulose – also has the highest change in mean positron lifetime.

ZUSAMMENFASSUNG

In der vorliegenden Arbeit wurden reine Zellulose und Papiermaterialien während der Wasseraufnahme und die damit einhergehende Änderung der Porengröße in den Materialien untersucht. Die Wasseraufnahme dieser porösen Materialien ist, aufgrund ihrer möglichen Anwendungen, ein interessantes Phänomen, dessen grundlegende atomare Prozesse noch nicht eindeutig festgestellt werden konnten. Im Folgenden wird die Methode der Positron-Annihilations-Lebensdauer-Spektroskopie (PALS) verwendet. Diese ist nicht destruktiv ist und eignet sich besonders zur Untersuchung von Porenvolumen und Porosität von Materialen. Zusätzlich zur verwendeten PALS-Methode, wurden Kontaktwinkelmessungen sowie Messungen des Wassergehalts in den Proben durchgeführt.

In dieser Diplomarbeit wurde die Positronenlebensdauer aller untersuchten Proben (reine Zellulose, Feinpapier und Kraft Sack Papier) während eines Be- und Entfeuchtungszyklus gemessen. Mithilfe der verwendeten PALS-Methode sollten während dieses Prozesses die Porengröße der Proben detektiert werden. Die PALS-Daten wurden im Programm PALSfit ausgewertet.

Diese Messungen zeigen einige interessante Ergebnisse; zum Beispiel, dass die mittlere Positronenlebensdauer mit dem Wassergehalt in den Materialien, wie erwartet, steigt. Das Interessante daran ist, dass der Anstieg der mittleren Positronenlebensdauer deutlich länger anhält als der Anstieg des Wassergehalts in den Proben.

Außerdem konnte gezeigt werden, dass die Änderung der Porengröße durch die Wasseraufnahme bzw. Trocknung reversibel ist; das bedeutet, dass die mittlere Positronenlebensdauer vor dem Befeuchten und nach dem Trocknen gleich groß ist.

Die PALS-Messungen zeigten außerdem für reine Zellulose und Kraft Sack Papier zwei Plateaus der mittleren Positronenlebensdauer in Abhängigkeit der Zeit. Das legt nahe, dass es zwei Wasseraufnahmeprozesse in diesen Materialien gibt, die zu verschiedenen Zeitpunkten stattfinden. Darüber hinaus zeigen die Ergebnisse, dass Zellulose, das Material mit der höchsten Wasseraufnahme, auch die größte Änderung in der mittleren Positronenlebensdauer aufweist.

CONTENTS

1 INTRODUCTION

The atomistic processes during water intake in different materials have always been an interesting phenomenon which is still point of discussions. Especially for materials with cellulose content the water sorption behaviour is extremely important for their product performance. In order to gain a deeper understanding in the ongoing processes in cellulose materials during water sorption the present thesis deals with the change of pore sizes in these materials while moistening. The method applied to measure the pore size is Positron Annihilation Lifetime Spectroscopy (PALS). It is a non-destructive method which is sensitive on open volume defects. On that account, the applied PALS method is a very suitable tool to investigate pore structures and crystalline structures in materials. This method does not only allow to predicate the pore size in the cellulose material, like differential scanning calorimetry [1] or Fourier transform-infrared spectroscopy [2,3] do, but gives also evidence to the relative changes in pore size.

The materials investigated do not have crystalline structures and therefore no regular structural units or vacancies in the material. Based on that, an investigation of dry cellulose using PALS, without a complimentary method, is very demanding.
Yet there are not many investigations of cellulose materials using PALS because this method is typically used for metals and materials with a crystalline structure. But former works already showed that PALS is also a powerful technique to analyse structures in porous materials [4]. On that account, it seems reasonable to address this complex matter and investigate paper and cellulose samples during moisture intake by the means of positron annihilation lifetime spectroscopy.

Earlier applications of PALS on cellulose materials [2,5] did not include the moisture intake in these materials. Hence, the aim of the present work is to investigate the influence of moisture intake on pore sizes in cellulose materials. For that purpose, three different cellulose materials with different cellulose, hemicellulose and lignin content were probed. The samples

investigated were pure cellulose, fine paper, which consists mainly of cellulose and hemicellulose and Kraft sack paper which contains additionally to cellulose and hemicellulose also lignin. Due to the different compositions and water affinity of these materials different water sorption behaviours are to be expected.

To associate the changes in pore size with the current water content in the samples, the weight of the samples during moistening is monitored. Additionally, contact angle measurements were carried out to give evidence to the wettability of each sample.

THEORETICAL PART

2 FUNDAMENTALS

2.1 ANTIMATTER

According to quantum field theory every particle in the standard model of particle physics has an antiparticle [6]. The antiparticle has the identical properties as the origin particle except for the electrical charge, the magnetic moment and all corresponding quantum numbers. Thus, antiparticles distinguish from their corresponding particles only in the case of leptons and quarks. For particles without electrical charge and magnetic moment particle and antiparticle are identical (e.g. for photons). The first antiparticle that was postulated and proven experimentally was the antiparticle of the electron, the anti-electron or positron [7].

The relationship between the momentum $\vec{p}$ and the energy *E* of a free particle, can be described by

$$\mathrm{E}^2 = \vec{\mathrm{p}}^2\mathrm{c}^2 + \mathrm{m}^2\mathrm{c}^4 \qquad (1)$$

where *c* denotes the speed of light and *m* the mass of the particle [8]. In the absence of an electromagnetic field, the solution for an electron of Dirac's equation leads to an energy spectrum with two bands, which are separated by an interval $2mc^2$. One of these bands corresponds to negative energy states $E = -c\sqrt{\vec{p}^2 + m^2c^2}$, the other one to positive energy states $E = +c\sqrt{\vec{p}^2 + m^2c^2}$. Dirac interpreted this, seemingly unphysical solutions, by a theory of holes, predicting a positive electron – the positron [9].

Then, in 1932 Carl David Anderson observed positively charged cosmic particles in a vertical Wilson chamber. According to his results, these particles had a lower mass than protons and were produced as secondary particles from radioactive decays, the experimental proof for the existence of positrons was found [10]. For this discovery he was awarded with the Nobel prize in 1936 together with the Austrian physicist Victor Franz Hess.

Over the next few decades antimatter became an important research field in physics. In 1955, Emilio Segrè and Owen Chamberlain at the University of California, Berkeley, discovered the antiproton and the antineutron, for which they were awarded the Nobel Prize in Physics in 1959 [11]. In the following decades, also the antiparticles of other subatomic particles were created in particle accelerator experiments (e.g. the antiproton in the Bevatron in the Lawrence Berkely National Laboratory or the antineutron by Bruce Cork et al.).

2.2 POSITRONS

The positron, which is the antiparticle of the electron, is a leptonic particle (as the electron itself). As all other leptons, the positron participates in gravitational and weak interaction and due to its electrical charge also in electromagnetic interactions. However, as the positron also belongs to the group of fermions, it does not participate in strong interactions [8].

The fundamental difference between the electron and the positron is the sign of their charge and all properties in connection to that. For example, the orbital and spin magnetic moments of the electron are antiparallel, while those of the positron are parallel to each other. In table 1 the most important properties of the electron and the positron are listed.

Contrary to electrons, positrons do not exist naturally except in very small numbers and for short times. They can be produced by radioisotope decay or by pair production of γ-rays, which will be further explained in section 1.5 [8].

Table 1: Properties of the electron (e^-) and the positron (e^+) with $e = 1.602 \cdot 10^{-19}$ As and $\hbar = 1.054 \cdot 10^{-34}$ Js

	positron e^+	electron e^-
charge	+ e	- e
resting energy m_e	0,511 MeV	0,511 MeV
radius r_e	$2{,}818 \cdot 10^{-15}$ m	$2{,}818 \cdot 10^{-15}$ m
spin s	ħ/2	ħ/2
magnetic moment	$+\mu_B$	$-\mu_B$
lepton number	-1	+1

It is worth mentioning, that the positron in vacuum is a stable particle like neutrinos, photons and electrons, all other particles are not stable in an isolated state and decay after a certain time. In nature, the positron loses its kinetic energy when in contact with matter due to thermalization and then annihilates with electrons under emission of γ-rays. The mean lifetime of positrons in condensed matter is in the range of 0.1 ns to 1 ns, in gases it is about 100 ns [12].

2.3 ANNIHILATION OF POSITRONS

The positron-electron annihilation process occurs as a 2-photon-annihilation or as a 3-photon-annihilation due to conservation of charge parity.

If an electron and a positron annihilate in a 2-photon-annihilation process, two γ-rays are emitted. The angle between these two γ-rays is 180°, as can be seen in figure 1a.

$$\mathrm{e^+ + e^- \rightarrow 2\gamma} \tag{2}$$

The corresponding energy is

$$\mathrm{E = 2m_e c^2 + E_+ + E_-} \tag{3}$$

with $m_e c^2 = 511\ \mathrm{keV}$ the resting energy of the electron (or positron), E_+ the kinetic energy of the positron and E_- the kinetic energy of the electron.

A 2-photon-annihilation occurs when the singlet-electron-positron-system has an antiparallel spin orientation, while in a 3-photon-annihilation-system, which is a triplet-electron-positron-system, the spins are parallel orientated. In this case, as the name suggests, three γ-rays are emitted, like shown in figure 1b. The three-photon-emission occurs much rarer and plays only a subordinate role (ratio of 3γ to 2γ-annihilation 1/372) [12].

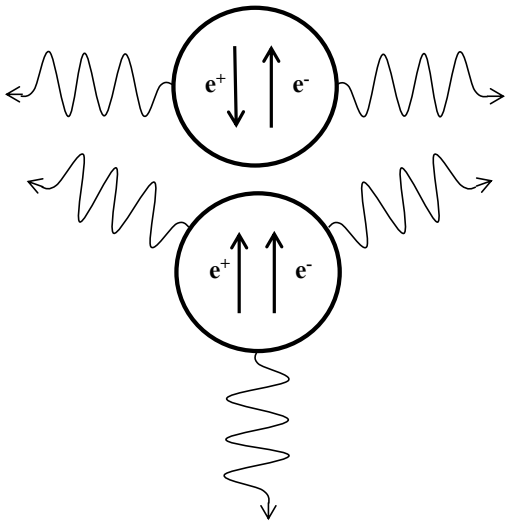

Figure 1: Top: (a) 2-photon-annihilation of singulett electron-positron system
Bottom: (b) 3-photon-annihilation of triplett electron-positron system

2.4 POSITRONIUM (Ps)

In 1944, Pirenne [13] and Wheeler [14] observed, that there is a possible bound state between a positron and an electron. The so-called positronium atom is stabilized by the electromagnetic interactions between the electron and the positron, with a binding energy of 6.8 eV. The lifetime of positronium, before the positron and the electron annihilate with each other, is in the range of nanoseconds. Positronium has been used to investigate the basic principles of quantum electrodynamics [15].

Depending on the spins of the participating electron and positron, there are two types of Ps: In the case of para-positronium (p-Ps) the spins of the electron and the positron are antiparallel to each other, while for ortho-positronium (o-Ps) the spins are parallel.

The p-Ps atom annihilates under the emission of two γ-quants and has a lifetime of about 0.125 ns. On the other hand, the o-Ps atom sends out three γ-quants when it annihilates and has a much longer lifetime of approximately 140 ns. The ratio between the number of o-Ps and p-Ps formation is given by the possible quantum numbers in which these two systems can appear. The statistical weight of a triplet state ($2J_T + 1 = 3$) is three times higher than the statistical weight of a singlet state ($2J_S + 1 = 1$). That means that three times more o-Ps than p-Ps is formed.

The p-Ps atom annihilates in condensed matter mainly through self-annihilation, while for o-Ps there is also another annihilation process, the so-called pick-off annihilation. This process is a 2-photon-annihilation with a further electron within the solid, which is not the electron in the Ps and has a spin antiparallel to that of the positron. Pick-off annihilation reduces the lifetime of o-Ps drastically to 1-10 ns. In table 2 the most important properties of o-Ps and p-Ps are compared.

Table 2: Properties of o-Ps and p-Ps

with $m_e = 9.109 \cdot 10^{-31}$ kg and $a_0 = 5.292 \cdot 10^{-9}$ cm

	mass	size	spins	total spin	lifetime	annihilation
o-Ps	$2 \cdot m_e$	$2 \cdot a_0$	↑↑,↓↓	1	142 ns	3 γ-rays
p-Ps	$2 \cdot m_e$	$2 \cdot a_0$	↑↓,↑↓	0	0.125 ns	2 γ-rays

2.5 POSITRON SOURCES

Positrons can either be formed as a product of radioactive decay or by pair production, where a high energy photon is converted in an electron-positron pair (see figure 2). To enable pair production, the energy of the photon must be higher than 1022 keV, which is given by the resting energy of the electron-positron pair ($2mc^2$ = 1022 keV) and for momentum conservation the presence of another particle is necessary.

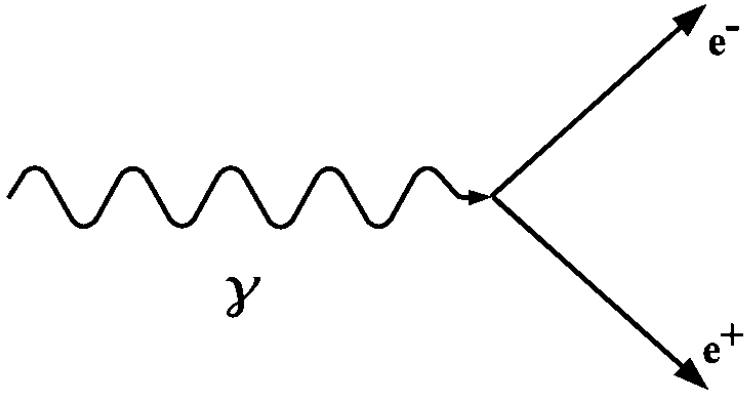

Figure 2: Schematic sketch of the pair production process where a high energy γ-ray is converted into an electron-positron pair.

Another possibility to generate positrons is the radioactive β^+-decay, where a proton (2 up-quarks, 1 down-quark) decays into a neutron (1 up-quark, 2 down-quarks). That means, an up-quark converts into a down-quark while emitting a positron e^+ and an electron-neutrino ν_e, to conserve the lepton number.

$$^{(1,1)}\mathrm{p} \rightarrow {}^{(1,0)}\mathrm{n} + \mathrm{e}^+ + \nu_\mathrm{e} \tag{4}$$

Radioactive elements which undergo a β^+-decay and have reasonable lifetimes are for example ^{22}Na, ^{58}Co or ^{64}Cu. The most commonly used radioactive isotope is the sodium isotope ^{22}Na. It has a good positron yield of about 90 % and its half lifetime is rather short with 2.6 years and it decays into an excited state of Neon (^{22}Ne*). The excited ^{22}Ne* then relaxes into the ground state sending out a γ-ray with an energy of 1.28 MeV [16].

$$^{22}\mathrm{Na} \rightarrow {}^{22}\mathrm{Ne}^* + \mathrm{e}^+ + \nu_\mathrm{e} \tag{5}$$

$$^{22}\mathrm{Ne}^* \rightarrow {}^{22}\mathrm{Ne} + \gamma \tag{6}$$

2.6 POSITRONS IN CONDENSED MATTER

Positrons entering condensed matter are slowed down to thermal energies [17] due to inelastic scattering with conduction electrons and phonons within a few picoseconds [18]. Before they annihilate, the thermalized positrons, diffuse through the matter; this process can be described by the parameter of the diffusion length *L* which is given by

$$\mathrm{L} = \sqrt{6\mathrm{D}_{+}\tau} \tag{7}$$

where τ is the lifetime of a positron in matter (~100-200 ps) and *D* is the diffusion constant. Typical diffusion lengths are in the order of about 100 nm (10^{-7} m). In matter positrons annihilate with electrons with a corresponding annihilation rate λ which is the reciprocal value of the positron lifetime τ and is defined as

$$\lambda = \tau^{-1} = c\pi r_0^2 \int \mathrm{n}_{+}(\mathrm{r})\mathrm{n}_{-}(\mathrm{r})\gamma(\mathrm{n}_{-})\mathrm{dr}. \tag{8}$$

It is determined by the overlap of the density functions $n_+(r)$ of the positron and $n_-(r)$ of the electron, as well as r_0 the electron radius and $\gamma(n_-)$ which describes the enhancement of $n_-(r)$ in vicinity of a positron [19].

Equation (8) shows that the lifetime of positrons is specific for a material due to the dependence on the electron density. Furthermore, when a material has pores, grain boundaries or other defects, there is additional free volume in the material. The lower electron density in these regions leads to a longer lifetime of the positrons in materials with larger pores and defects. Figure 3 shows a schematic sketch of positron penetration in a material.

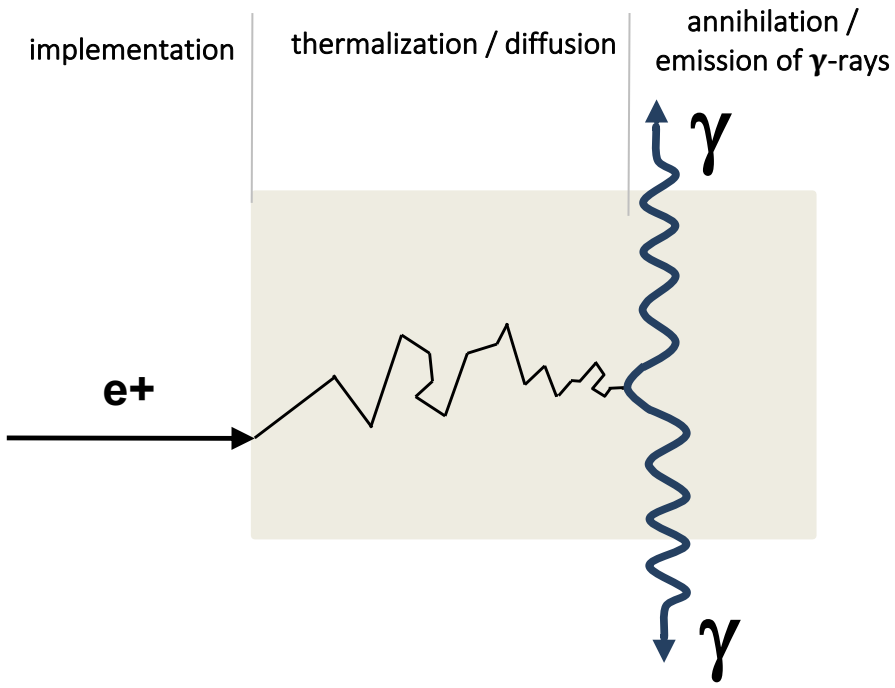

Figure 3: Schematic sketch of a positron implantation in a material. At first the e^+ is implanted into the material, where it slows down to thermal energies and diffuses through the material until it annihilates with an e^- under the emission of γ-quants.

2.6.1 TRAPPING MODEL

As a positron diffuses through a solid it can either annihilate within the defect-free bulk of the material with a lifetime τ_b or it can be trapped at a defect and annihilate there with a lifetime τ_d. Due to the absence of positively charged ions within these defects, positrons experience an attractive potential and get trapped with a trapping rate κ.

Since the electron density in the defect is lower than in the bulk of the solid, the positron lifetime corresponding to annihilations in defects τ_d is longer than the lifetime τ_b corresponding to annihilations in the bulk. To illustrate this, figure 4 shows the scheme of the trapping model with one specific type of defect.

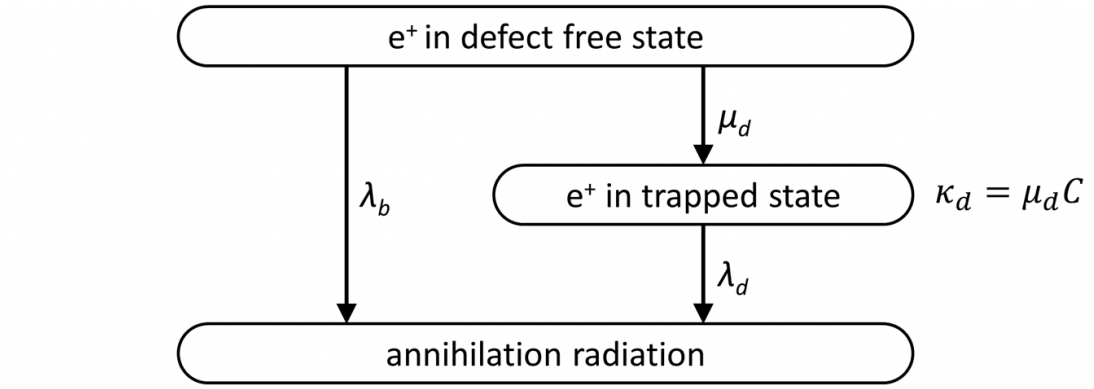

Figure 4: Scheme of the trapping model with one defect type [20]. Positrons can either annihilate in the bulk with the annihilation rate λ_b or get trapped in a defect with trapping rate μ_d where they annihilate with the annihilation rate λ_d.

The trapping rate κ can be derived by Fermi's golden rule as

$$\kappa = \frac{2\pi}{\hbar}\sum_{i,f} P_i M_{if}^2 \delta(E_i - E_F) \tag{9}$$

with *i* the initial state with energy E_i, *f* the final state with energy E_F and M_{if} denotes the transition matrix between the states *i* and *f*, P_i is the occupation probability [21]. The final state describes a trapped positron in a defect and the initial state is a delocalized Bloch state of a positron. The trapping rate κ is proportional to the defect concentration *C* in the solid:

$$\kappa = \mu C \tag{10}$$

where μ denotes the specific trapping rate [22]. Assuming only one type of defect exists in the material, one can derive the number of positrons in the material after a time *t*

$$n(t) = n_b(t) + n_d(t) = I_1 \exp\left[-\frac{t}{\tau_1}\right] + I_2 \exp\left[-\frac{t}{\tau_2}\right] \tag{11}$$

where n_b and n_d describe the density of positrons in the bulk (free state) and in the defect (trapped state). Here, τ_i denotes the individual lifetime components and I_i the corresponding intensities [20]. The intensities I_1 and I_2 add up to 100%; mathematically expressed that means

$$I_1 = 1 - I_2 \tag{12}$$

$$I_2 = \frac{\kappa_d}{\lambda_b - \lambda_d + \kappa_d} \tag{13}$$

with κ_d the trapping rate in defects, λ_b and λ_d are the annihilation rates in bulk and defects, respectively. The individual lifetime components can be expressed with those parameters as follows:

$$\tau_1 = \frac{1}{\lambda_b + \kappa_d} \tag{14}$$

$$\tau_2 = \frac{1}{\lambda_d} \tag{15}$$

The total annihilation probability can be measured experimentally. It is calculated via the time derivation of equation (11) which is

$$|P(t)| = \left|\frac{dn(t)}{dt}\right| = \frac{I_1}{\tau_1}\exp\left[-\frac{t}{\tau_1}\right] + \frac{I_2}{\tau_2}\exp\left[-\frac{t}{\tau_2}\right] \tag{16}$$

From equation (14) one can see, that in the case of one defect, the annihilation probability, which is the spectrum observed in the experiment, consists of two exponential decays. I_2 is the defect-related intensity. If there are less defects, I_2 becomes smaller and the spectrum only depends exponentially on τ_1 which corresponds to the bulk lifetime of the positron in the material [20].

The most important parameter to compare relative changes in defect concentrations is the mean positron lifetime $\bar{\tau}$ which is for (n-1) defect types given by

$$\bar{\tau} = \int_0^\infty P(t)dt = \frac{1}{n}\sum_{i=1}^{n} \tau_i I_i. \tag{17}$$

It is a very stable parameter since it is in most cases not sensitive to the applied fitting procedure. For this reason, the mean positron lifetime was chosen as ideal parameter to monitor changes of pores or moisture content in the very complex and inhomogeneous cellulose materials which is the aim of this thesis.

2.6.2 FORMATION OF POSITRONIUM

If a positron enters a solid it is, under certain conditions, energetically more favourable to form positronium than to annihilate with surrounding electrons immediately.

Positronium can either be created in the bulk or at the surface of a material. If positronium is formed in the bulk of a material it can either annihilate, be trapped in a defect or diffuse

through the material and be emitted at the surface if its energy is still sufficient. If an implanted positron reaches the surface of a material, it is, for certain materials, energetically more favourable to capture an electron and leave the solid as a positronium atom than to be emitted directly without the formation of positronium.

Whether bulk or surface formation of positronium is favoured depends on the defect characteristics and electron densities of the solid. For example, in metals positronium is usually not formed in the bulk of the material because Coulomb interactions between electrons and positrons are screened by the high number of free electrons. However, due to the high number of available surface states, positronium can be created at the surface of metals quite efficiently [23].

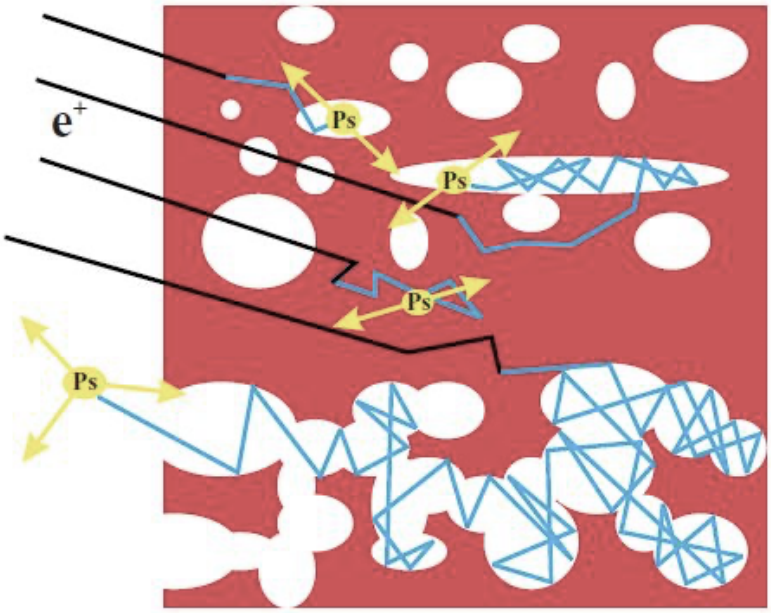

Figure 5: Positrons in porous matter [4]

For insulators, Ps bulk formation is more likely than surface formation due to a lower electron density. Also, in porous materials with many defects positronium is mainly formed in the bulk. For characterization of porous materials especially the ortho-Ps formation in defects is important [24].

Due to the high number of free open volumes in porous materials compared to crystalline ones, the probability to form o-Ps is higher because it is more likely to be formed in defects than in the bulk. In general, this leads to a longer mean positron lifetime τ_{mean} according to the longer lifetime of o-Ps.

The possible processes which can occur when a positron enters porous matter are shown in figure 5. After the positron penetrates a porous material, its energy slows down to the range of thermal energies and it diffuses through the material. After diffusion, it can either annihilate with an electron in the bulk, form Ps in the bulk, form Ps in an open volume, or diffuse to the surface and form Ps there. The timespan until annihilation occurs, is longer if Ps formation occurs. Additionally, the “trapping” in the free open volume contributes to a longer mean lifetime of the positron.

2.7 POSITRONS IN LIQUIDS

Due to large discrepancies of the structural properties of liquids and solids, it is not reasonable to describe positrons in liquids by the trapping model. To describe the behaviour of positrons in liquids, it is common to use the so-called bubble model.

2.7.1 BUBBLE MODEL

The three different processes which a positron can undergo when it enters a material are: the formation and annihilation of p-Ps corresponding to the shortest lifetime (τ_1), the annihilation of the positron without forming Ps (τ_2) and the formation of o-Ps which results in general in the longest lifetime component (τ_3). In liquids o-Ps tends to push out surrounding molecules to form a so-called Ps-bubble. The overlap of the surrounding electron wave function and the o-Ps wave function corresponds to the pick-off rate of the surrounding electrons. In the bubble model the lifetime τ_3 depends on the Ps-bubble radius. The radius is influenced by the surface tension of the surrounding liquid which depends among others on the surrounding temperature. Water, for example, has a decreasing surface tension when the temperature is increased, that means that τ_3 would be longer for higher temperatures [25]. Another common theory to describe positrons in liquid is the so-called blob model which was first described by Stepanov et al. [26].

2.8 APPLICATION OF POSITRONS IN MATERIALS SCIENCE

To investigate the defect structure of a material, the method of positron annihilation spectroscopy can be applied. An outstanding advantage of the use of positrons for the investigation of defects is their enormous sensitivity; furthermore, the method is non-destructive.

The spatial probability density of positrons in a material shows that they are strongly localized at the defects due to the missing positively charged, repelling nucleus at these sites [27] which is the reason for positrons being a successful probe for the study of defects.
Depending on which information of the annihilation γ-quants is further analysed, three types of positron annihilation techniques can be distinguished:

- Positron annihilation lifetime sepctroscopy
- Doppler broadening spectroscopy
- Angular correlation spectroscopy

All of these methods are based on the same principle, namely the emission of γ-quants when a positron or a positronium annihilates. For the present thesis, the applied method is positron annihilation lifetime spectroscopy which has been described in detail in the proceeding paragraphs of this chapter.

2.9 CELLULOSE

Cellulose was discovered by Anselme Payen in 1838, he extruded it from plants and determined the chemical formula [28,29,30]. Natural sources for cellulose are plants, for example cotton consists of approximately 90% cellulose, while wood has a cellulose content of 40-50% [31,32]. On Earth, cellulose is the most numerous organic polymer.

2.9.1 STRUCTURE

Cellulose is a polysaccharide, consisting of a linear chain with hundreds to thousands of D-glucose units. The chemical formula of these units is $(C_6H_{10}O_5)_n$, their structure can be seen in figure 6. There are several processes to produce cellulose for example biosynthesis, where it is extracted from plants and the cellulose fiber is dissolved in nitric acid and acetic [33].

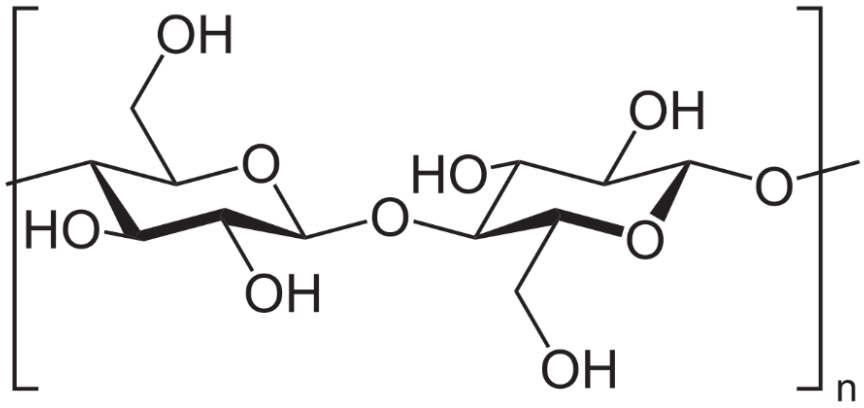

Figure 6: Chemical structure of one cellulose unit (D-glucose unit) [34]. O denotes the oxygen atoms which act as a glycosidic linkage which holds the chains in cellulose together and OH represent the hydroxyl groups.

2.9.2 PROPERTIES

Cellulose is white, hydrophilic, insoluble in water, a straight chain polymer and biodegradable. It has been shown that cellulose can be melt at 740 K [35]. As already mentioned, it consists of D-glucose units. The hydroxyl groups on the glucose form hydrogen bonds with the oxygen atoms in the cellulose which holds the chains together (glycosidic linkages, compare with figure 9).

Depending on the different locations of hydrogen bonds in cellulose, different crystalline structures can be distinguished: cellulose I is the natural cellulose, cellulose II is in regenerated cellulose fibers, further there are cellulose III and IV which can be generated with chemical treatments [36]. The degree of polymerization, which is the number of basic elements in a polymer chain [37], and the chain length influences the properties of the cellulose.

2.9.3 LIGNIN IN CELLULOSE MATERIALS

Most cellulose is obtained from cotton and wood pulp. Plants have another major component besides cellulose – lignin. For example, wood contains approximately 40% to 50% cellulose and 20% to 30% lignin. To separate lignin from cellulose, the Kraft process is used. In this process wood is converted into wood pulp, which consists of almost pure cellulose. It is the dominant process for producing paper, where wood chips are added to a mixture of sodium hydroxide (NaOH), sodium sulphide (Na_2S) and hot water. This leads to a break of the bonds which link cellulose, hemicellulose and lignin.

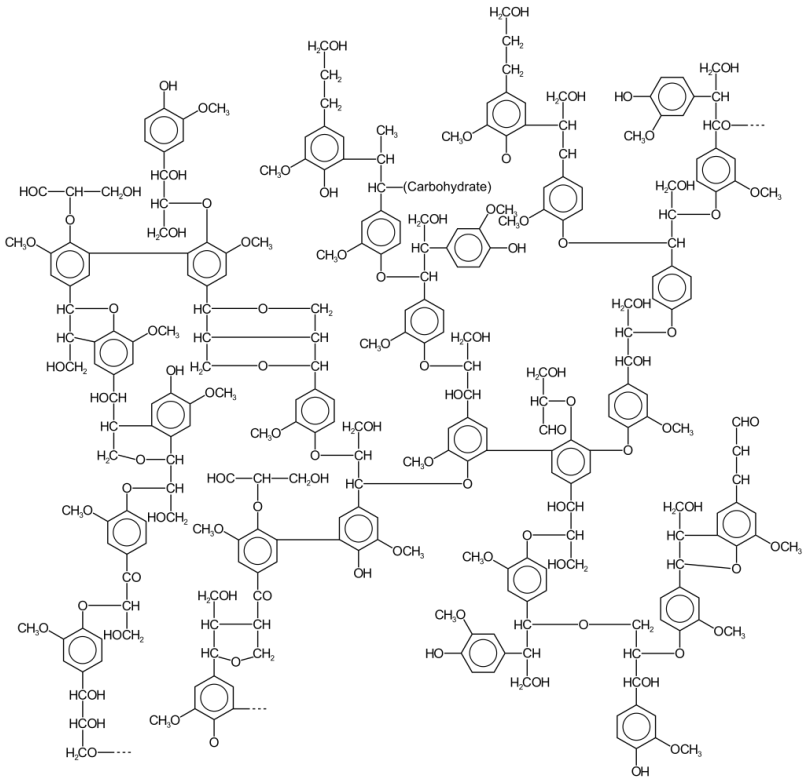

Figure 7: Possible chemical structure of lignin [38]. In general, it is a class of complex three-dimensional structures of phenolic polymers which vary from species to species.

Lignin is also an organic polymer which is of brown colour. It is, contrary to cellulose, hydrophobic and has many aromatic subunits. Especially in plants lignin is important for cell walls because it does not rot easily and lends the walls their rigidity. The composition can be various, there is no defined primary structure, one possible arrangement is shown in figure 7. It is a cross-linked polymer, with three main types of cross link: 4-hydroxyphenylpropane, 3,5-dimethoxy-4-hydroxyphenylpropane and 4-hydroxy-3-methoxyphenylpropane.

2.9.4 APPLICATION

A few typical applications for cellulose materials are paper products, fibers for textiles, microcrystalline cellulose as inactive filters, insulation material in buildings [39] and as electrical insulation paper. The possible field of application for cellulose is very widespread.
In the present thesis, the analysed samples are different papers and pure, chemically synthesized cellulose. Different paper products vary due to their cellulose and lignin content. For example, Kraft paper has a high amount of lignin which is the reason for its brown colour. In contrast, fine paper has a very low (< 5 %) lignin content.

2.9.5 TRANSPORT OF LIQUIDS IN CELLULOSE

Transport of water in papers and cellulose is of big interest for the paper industry. In general, the moisture sorption characteristics of hygroscopic materials are of high importance due to the big influence on the material properties. Since cellulose is hydrophilic and lignin is hydrophobic, the content of lignin in a cellulose material influences the behaviour of water sorption strongly.
In porous materials, like cellulose, pore size and shape have a big influence on the properties. Moisture uptake changes the pore size distribution in the material. In natural cellulose, pores are already present in the fibers and can additionally be generated by mechanical and chemical treatments. There are several theories of sorption mechanisms like cluster formation and layered adsorption which influences the pore size distribution [3]. Water is potentially being adsorbed at the position of the hydrophilic carboxyl and hydroxyl groups in the cellulose fiber. An exact analysis of the pores and change of the pore size due to moisture intake is very complex and has already been investigated with different methods. For

example, with differential scanning calorimetry (DSC) [1], scanning electron microscopy (SEM) [40], light scattering [41] and Fourier-transform infrared spectroscopy [3]. From these experiments it is clear to see that the moisture sorption in cellulose materials occurs in a very uniform manner. It could also be shown that the moisture uptake at the carboxyl groups is faster than that on the hydroxyl groups at high humidity. It is also worth mentioning, that in the drying process the fiber walls start to collapse at larger pores followed by a collapse of smaller pores.

It is well known, that the pore size is changing during sorption and drying processes in cellulosic and paper materials. There is a specific term which describes the chemical and physical changes in the cellulose fibers, such as the shrinking of the pore volume while drying – the so called “hornification”. It was introduced to the papermaking literature by G. Jayme in 1944 [42,43].

2.10 METHODS

In this section the experimental methods used are shortly explained. Besides the already described PALS also contact angle measurements and detection of the relative mass were conducted.

2.10.1 POSITRON ANNIHILATION LIFETIME SPECTOSCROPY IN CELLULOSE MATERIALS

Positron Annihilation Lifetime Spectroscopy is frequently used to investigate crystalline materials, like metals. More infrequent it is used to investigate porous materials, but recent works showed that PALS in porous materials provides reasonable findings [4].
In porous materials, like cellulose and paper materials, positronium tends to annihilate more frequently into three photons (ortho-Ps) instead of two photons (para-Ps) compared to non-porous materials. Due to the much longer lifetime of o-Ps (~ 142 ns), which is more often formed and trapped in closed pores, compared to the rather short lifetime of p-Ps (~ 0.125 ns, see section 1.4), the mean lifetime of the positrons in the sample increases with porosity of the sample. Applying PALS the behaviour of positronium formation can be detected quantitatively because a positron spectrum contains several signature lifetimes which correspond to annihilation at different trapping sites. Typically, in porous materials more than two lifetime components are detected, some of these components can be pore-sensing and give evidence to the pore size and distribution in the material. In general, one or more lifetime components correspond to annihilation in pores. The lifetime gives information about the pore size; while the intensity of the lifetime depends on the porosity and how many pores are in the material. A model which describes the behaviour of positrons in pores quantum mechanically was developed by Tao [44] and Eldrup et al. [45]. In this model positronium which is localized in an infinitely deep potential well, only undergoes pickoff annihilation with electrons from the molecule when it is near the pore surface. With the assumptions in the model one can calculate the pickoff annihilation rate $\lambda_{pickoff}$ for a given pore size. The total positronium decay rate λ can then be calculated with

$$\lambda = \lambda_{\mathrm{pickoff}} + \lambda_{\mathrm{vacuum}} \tag{18}$$

where λ_{vacuum} denotes the vacuum decay rate of o-Ps which is 1/(142 ns).

The Tao-Eldrup model only takes into account the ground state of o-Ps. That is the reason why the model is not sufficient for larger pores, more specifically when the pore diameter exceeds the De Broglie wavelength of positronium which is approximately 6 nm [21].
Previous works of investigation cellulose using PALS have been done by Cao et al. [2] and Doyle et al. [5]. These works showed that the o-Ps lifetime and pore size are directly correlated with each other. These results suggest that the ortho-positronium prefers to form in pores and open volume defects. To show that, Cao et al. used ball milling to generate new holes in the cellulose with smaller size. They observed an increase of o-Ps intensity with milling time. They attributed this observation to the increase of the amorphous phase during ball milling. It could be shown as well that the o-Ps lifetime correlates directly with the hole size and the hole number with the corresponding intensity. Doyle et al. suggest that Ps-formation occurs in the free volume in the region between elementary fibers.

2.10.2 CONTACT ANGLE MEASUREMENTS

Contact angle measurements can be applied to extract information about the behaviour of cellulosic materials in contact with liquids and contact angles are frequently used to measure the wettability of a surface. This refers to the ability of the observed liquid to form boundary surfaces with matter. A small surface tension of the liquid leads to a small contact angle, while a high surface tension causes a high contact angle between the liquid and the material. This means that in the case of a smaller contact angle the cohesive forces are weaker than the adhesive forces. For large contact angles, the cohesive forces are stronger than the adhesive forces. Usually one speaks of a wetting liquid if the liquid forms a contact angle which is smaller than 90° and a non-wetting liquid is defined if the contact angle is between 90° and 180° [46]. Thomas Young defined the contact angle θ between a liquid and a surface as the equilibrium of a drop resting on a solid plane surface with consideration of three surface tensions:

$$\gamma_{lv} - \gamma_{sl} = \gamma_{sv}\cos\theta \tag{19}$$

where γ_{lv} denotes the interface between the liquid and the vapor phase, γ_{sl} describes the interface between the solid and the liquid phase and γ_{sv} between the solid and the vapor phase. All these quantities are shown in figure 8.

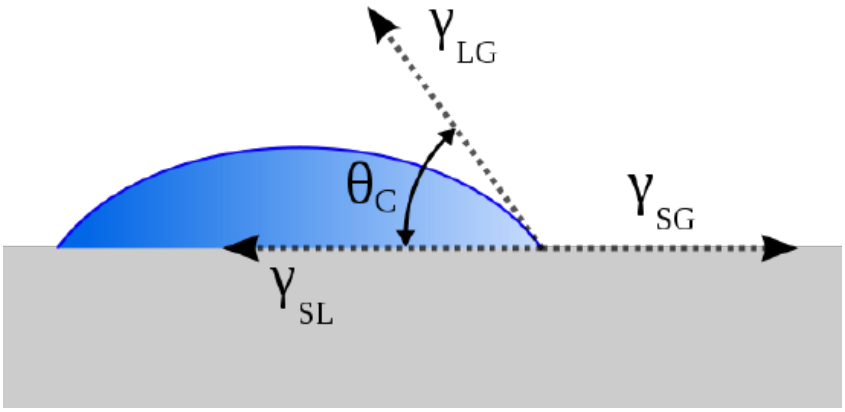

Figure 8: Contact angle and interfaces between the liquid, the vapor and the solid phase in a contact angle measurement [46].

To measure this contact angle a drop is set on the samples with a thin micro pipet very precisely. Then a photo of the droplet on the sample is taken with a high-resolution camera. In the last step this picture is analysed by a computer software which is able to measure the contact angle in the picture exactly.

2.10.3 DETECTION OF WATER CONTENT

The moisture content (MC) is defined by

$$\mathrm{MC} = \frac{\mathrm{m_w}}{\mathrm{m_c}} \tag{20}$$

with m_w the mass of water and m_c the mass of the cellulosic material. To determine the moisture content of the cellulosic material, the sample is placed into a humid environment and its mass is determined as a function of time. The difference in mass between the dry sample m_c and the wet sample is the water mass m_w.

EXPERIMENTAL PART

3 EXPERIMENTAL

The aim of this thesis is to investigate the change of pore size of cellulosic materials during moisture intake using positron annihilation lifetime spectroscopy (PALS). Complementary to the detection of the pore size with PALS, the water content of the material is detected by weighting the sample. To determine the wettability of the analysed samples also contact angle measurements were carried out.

3.1 INVESTIGATED MATERIALS

Three different types of cellulose materials were probed: pure cellulose and two sorts of paper with different cellulose and lignin content, namely fine paper and Kraft sack paper.

Cellulose

The investigated cellulose was produced by the company Kellheim fibres. It is an extremely flat viscose fibre of cellulose type II (see section 1.9.2), which is thermodynamically more stable than cellulose type I. The thickness is only one fortieth of the width, which means it is a very flat fiber. The cross-section is highly regular and the surface is very even. It is typically used for transparent papers [47]. Figure 9 shows a SEM picture of the fibre.

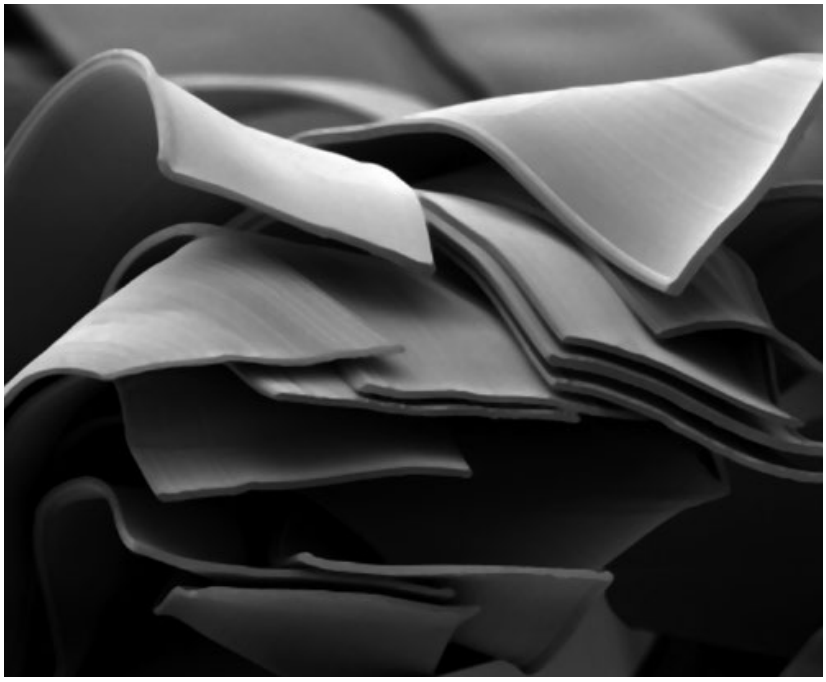

Figure 9: SEM picture of the investigated cellulose [47]

Fine paper

The area weight of the investigated fine paper is 90 g/m^2 (according to DIN EN ISO 536 Paper and board – determination of grammage), it is produced by the company Mondi. The used pulp for the production of the fine paper is eucalyptus but it also contains additives to achieve better properties for its applications. That means, besides cellulose and hemicellulose there is also other filling material. The filling material consists of carbonates, especially calcium carbonates. Most of the lignin which was originally in the pulp is removed to obtain the white colour of the paper (lignin gives paper a brown colour). The paper is typically used for commercial printing as well as book production. The roughness of the paper is very low with only 35 ml/min (according to ISO 8791-2:2013 Paper and board – Determination of roughness/smoothness (air leak methods) – Part 2: Bendtsen method), complimentary the smoothness is rather high with 207.5 s (according to ISO 5627:1995 Paper and board – Determination of smoothness (Bekk method)) [48]. Roughness, which is the degree to which the surface has fine irregularities [49], and smoothness are important parameters in paper manufacturing because they give information about the properties of a paper for e.g. printing.

Kraft sack paper

The investigated Kraft sack paper is also produced by the company Mondi and has an area weight of 70 g/m^2 (according to DIN EN ISO 536: Paper and board – determination of grammage). The pulp used for the production contains predominantly of spruce and also of pine. It is a brown extensible paper with very high porosity, runnability and tensile energy absorption [50]. Due to the fact that the lignin is not removed in sack papers, it is brown coloured. It is used for packaging, especially for packaging of cement and building materials, food and chemicals. The high tensile strength of approximately 5.7 kN/m [50] and the high porosity are especially necessary for the filling process of the cement bags. The cement is typically blown into the bags with high pressure, this demands that the air easily get through the bags while the cement is retained inside; this process requires a high tensile strength and high porosity.

3.2 EXPERIMENTAL SET-UP

In this section the experimental applied methods and corresponding set-ups applied in this thesis are briefly described.

3.2.1 POSITRON ANNIHILATION LIFETIME SPECTROSCOPY (PALS)

The chosen experimental method for investigation of the change of the pore structure in cellulose materials is positron annihilation lifetime spectroscopy. Single positrons emitted by a radioactive source are implanted into the sample. The lifetime of the positron in the material is measured as difference between a start signal, which is the 1,28 MeV birth γ-quant in the case of a ^{22}Na source, and a stop signal, which is the 511 keV γ-quant emitted due to the positron-electron annihilation. The start- and stop quants are detected with a fast-fast positron annihilation lifetime spectrometer. In figure 10 a block diagram of the setup is shown.

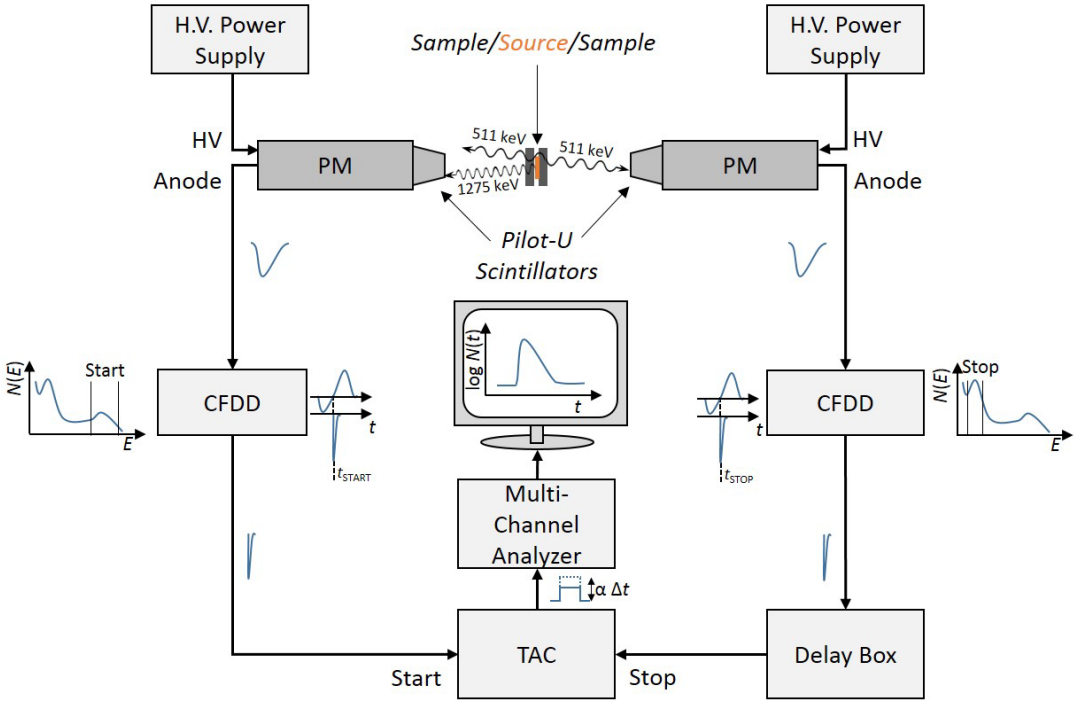

Figure 10: Block diagram PALS [20,51]: When the γ-quants from the sample-source-sandwich reach the scintillators, they are converted into photons of visible light which are transformed to an electrical pulse in the photocathode. These electrical pulses are amplified in the photomultiplier tubes. In the constant fraction differential discriminator (CFDD) a timing pulse is delivered when the electrical pulse is arriving. In the time to amplitude converter (TAC) an output voltage is generated proportional to a time difference.

To achieve a minimum distance between the positron-emitting source and the sample, the radioactive source is placed in between the two samples. This “source-sample-sandwich” is fixed with a wire in the case of the present experimental set-up. The positrons annihilate in the sample and emit γ-quants.

In the scintillator crystal the incoming γ-quants are converted into visible light and these photons are converted into electrical pulses at the photocathode and further amplified in the photomultiplier tube (figure 11, figure 10 PM). The energy of the γ-quant is proportional to the intensity of the pulse. In the constant fraction differential discriminator (CFDD) a timing pulse is delivered when the electrical pulse is arriving. One CFDD detects in the energy range of the start (birth) γ-quant, the other one in the range of the stop (annihilation) γ-quant. With a time to amplitude converter (TAC) an output voltage is generated which is proportional to the time difference between the start and stop quant. This output signals are transferred to an analogue-digital converter (ADC) and then stored in a multichannel analyser (MCA). These signals are transferred to the computer where they are analysed with the program PALSfit. To obtain a full lifetime spectrum a sufficient number of annihilation processes are necessary (~10^6 counts in a spectrum). Hence, the data from the single annihilation processes are stored.

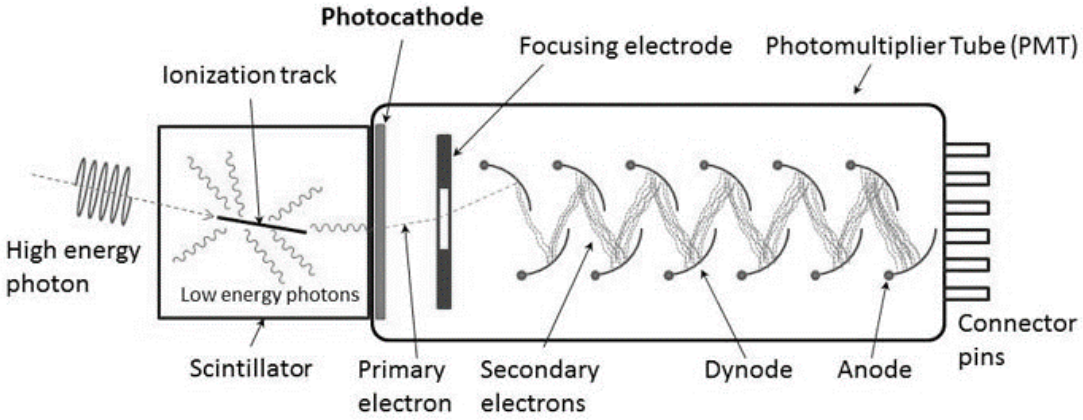

Figure 11: Scionix scintillator and photomultiplier. When a high energy photon enters a scintillator crystal that produces an electron that ionizes a track. This ionization process leads to an emission of lower energy photons. If these photons enter a photocathode, they knock electrons out according to the photoelectric effect. These knocked out electrons, the so-called primary electrons are focused to a beam via a focusing electrode. This beam is focused on a dynode where the electrons knock out secondary electrons. The number of electrons from dynode to dynode increases due to the higher voltage that is applied on every following dynode. After the dynodes, the electrons are guided to an anode, where they are conducted to connector pins.

In figure 12 a typical PALS spectrum is shown. The measured spectrum is a sum of exponential decays which is convolved with the time resolution function of the spectrometer superimposed with a constant signal from background radiation. Positron lifetime spectra include a prompt peak corresponding to short annihilation times, caused by positron and p-Ps annihilation followed by a decreasing signal. If there is a significant amount of o-Ps being generated in the sample, this leads to higher count rates in the region after the prompt peak and a less rapidly decreasing signal in this region (compare figure 12, orange curve: o-Ps formation in sample, black curve: no o-Ps formation).

The positron lifetime is indirectly proportional to the electron distribution function, as can be seen in equation (8). Specific materials have typical bulk positron lifetimes τ_b depending on their specific electron density. In general, materials with a lower electron density have higher bulk positron lifetimes than materials with a higher electron density.
The positron lifetime τ_d, corresponding to annihilations in open volume defects, depends on the size of the open volumes - the larger the open volume, the higher the positron lifetime - because open pore volumes support o-Ps formation due to a larger surface area where Ps-formation can take place. In a material with many defects there is also more Ps-formation in the bulk which can then be trapped in the open volumes. The intensity of the defect-related lifetime component τ_d contains information about the number of defects in the sample.

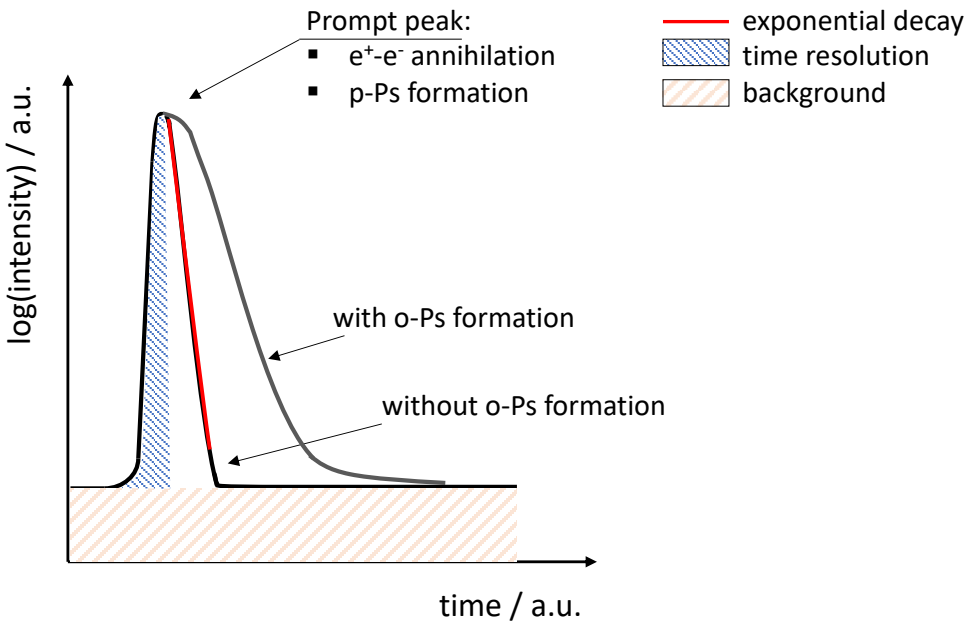

Figure 12: Typical shape of a lifetime spectrum. Due to the short annihilation time of positrons there is a prompt peak, followed by a decrease, which steepness depends on the amount of o-Ps formation. If there is o-Ps formation (orange curve), the mean lifetime of positrons in the sample increases due to the higher intensities at long lifetimes compared to the case where no o-Ps formation occurs (black curve).

Each cellulose material sample which was investigated using PALS, was measured within a certain cycle: At first, the “dry” sample was measured for approximately 1 day, after this the very same sample was measured in a “wet” state by changing the relative humidity to approximately 80 % and then it was “dried” with a relative humidity of less than 10 %. During this whole cycle, the positron lifetime of the sample was continuously monitored. The “wet” and “dried” measurements lasted approximately 4 days each. The reason for the extended measurement time is that the cellulose materials undergo long-term processes of water ab-, ad- and desorption while moistening and drying, respectively. The “dry” conditions mean laboratory conditions, which is related to approximately (50 ± 3) % humidity at a temperature of 20°C. The “wet” conditions at (80 ± 3) % relative humidity and the “dried” conditions of less than 10 % relative humidity also correspond to a temperature of 20°C.

To achieve the above described conditions, a box was designed where the sample was put during the measurements and the microclimate conditions could be set up. This box is shown in figure 13. The upper part of the box, which is named source-sample chamber in the following, where the sample and radioactive source is placed during the measurements, was printed by a 3D printer (see figure 14). Important for the design of the source-sample

chamber was the requirement that it should be as narrow as possible to minimize the distance between the sample and the detectors of the spectrometer. Another constraint was, that the source-sample chamber should be in direct contact with the rest of the box to ensure the same humid atmosphere. Furthermore, the ^{22}Na source should be safely fixed between the sheets of the sample paper without direct contact to the water. The humidity conditions of the "wet" measurement were set up placing a petri dish with water in the box. For the "dried" measurement the petri dish was filled with silica gel, respectively. For the "dry" measurement the petri dish was left empty and conditions of the surrounding laboratory could adjust.

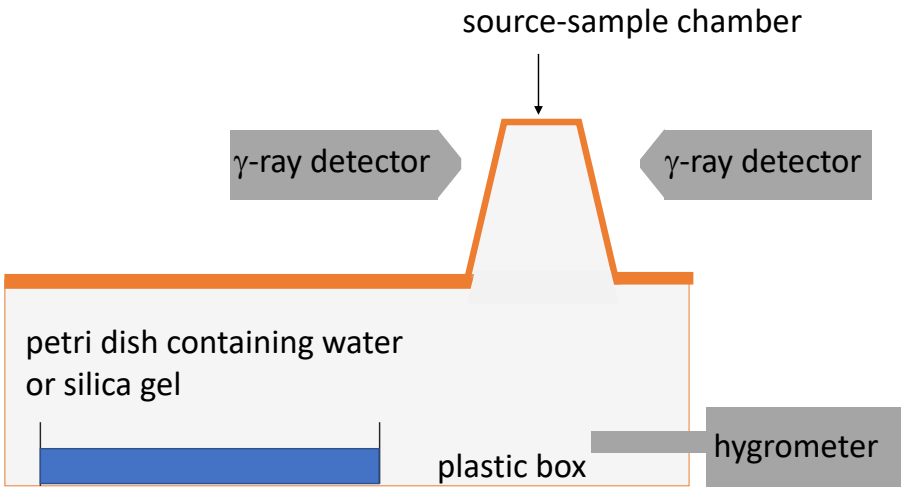

Figure 13: Experimental set-up of the sample container for PALS of cellulose material [52]. The source-sample chamber is fixed on the top of the plastic box and centred between the γ-ray detectors. Inside the box a petri dish is placed which is either filled with water ("wet" measurement) or silica gel ("dried" measurement). Additionally, the sensor of a hygrometer is placed inside the box to monitor the relative humidity during the measurement.

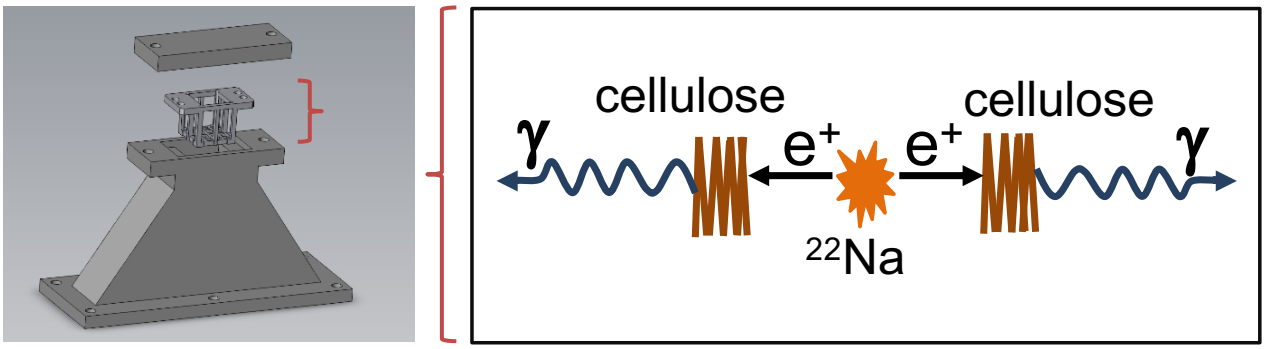

Figure 14: 3D-printed upper part – source-sample chamber (left) and sketch of the source-sample arrangement (right) [52].

On the right side of figure 14 a sketch of the arrangement of the source and the sample is shown. Due to the penetration depth of the positrons and the small thickness of the cellulosic materials, the cellulose sheets were folded (to approximately 20 sheets of cellulose on each side). The radioactive source was stack into one of the folded samples and on each side of this sample, another folded sample of the same material was added to achieve a wide sample depth. This was done to avoid that some of the positrons may annihilate after passing through the sample due to a larger penetration depth.

3.2.2 CONTACT ANGLE MEASUREMENT

Contact angle measurements were performed to investigate the wettability of the samples. The underlying principal was already described in section 1.10. The experimental set-up was rather simple: the samples were fixed on an object plate with adhesive tape to ensure an even surface. In the next step, a water drop of defined size was produced with a micro pipet on which this drop sticks. The defined size of the drop was achieved by two lines which were superimposed on the live high-resolution camera picture, these are the green lines in figure 15. The micro pipet was slowly moved towards the sample until the droplet retains on the sample. Subsequently, a photo was taken with a high-resolution camera and the contact angles were measured in this resulting photo by a computer software. The software used was KSV Contact Angle Measurement system. To achieve a high-quality picture with the camera, an infrared-emitting light source was placed behind the observed sample. This process was repeated to ensure a statistical analysis of the measured angles for each sample. A rough sketch is shown in figure 16.

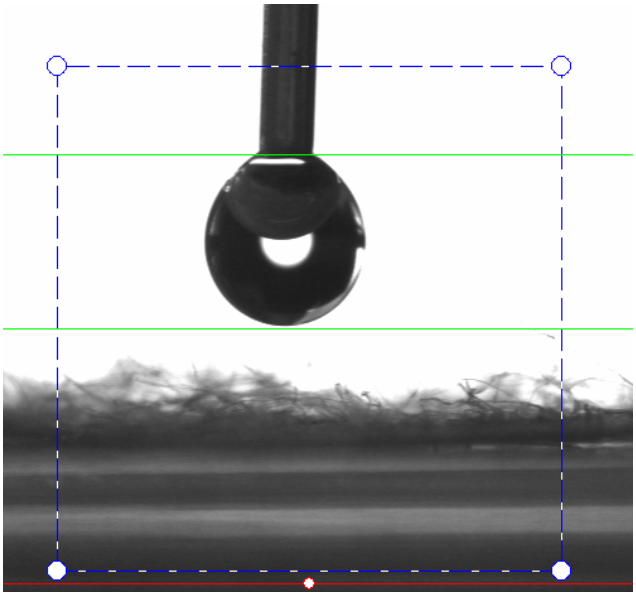

Figure 15: Picture of the high-resolution camera used for contact angle measurements: water droplet and micro pipet above paper sample. The green lines define the size of the water droplets.

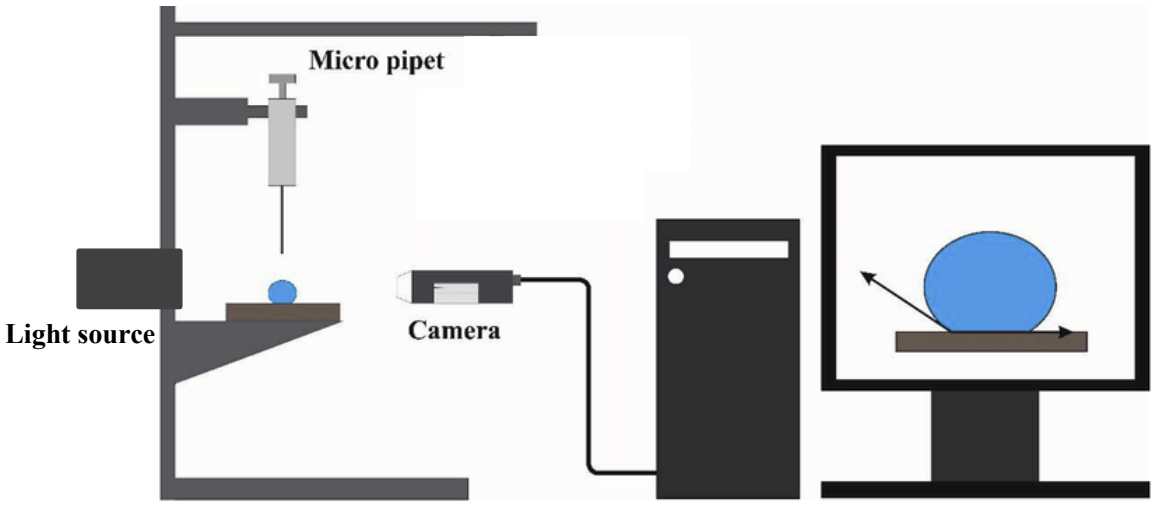

Figure 16: Experimental set-up of the contact angle measurement, adopted from [53].

3.2.3 DETECTION OF WATER CONTENT

To monitor the water content of the samples during moisture intake and to compare it with the positron lifetime data, the weight of a sample identical to the PALS sample was monitored in the very same humid atmosphere in a second experimental set-up identical to that used for the PALS measurement (see figure 13) except for the hygrometer.

In the case of the second experimental set-up for monitoring the water content, the radioactive source was not put in between the sheets of the sample, but the humid atmosphere was identical to that in the experimental set-up for the PALS measurement (Petri dish with same amount of water, same size, same outer box).
To determine the weight of the sample, the sample was weighted in defined time steps, in parallel to the PALS measurement and for the same period of time. The scale used is from the company Sartorius, the model MC21S, which is shown in figure 17, its accuracy is 1 μg.

Figure 17: Fine scale used for weighting the samples: Sartorius model MC21S

RESULTS AND DISCUSSION

4 RESULTS AND DISCUSSION

In the following chapter, the experimental results are presented, analysed and discussed. At the beginning, the results for cellulose, fine paper and Kraft sack paper are represented separately. For each sample the results of the PALS measurements, contact angle measurements and water content measurements are shown, in the order mentioned. Subsequently, a comparison of all three investigated samples is given and an outlook to possible further measurements for the investigation of cellulose materials with the methods used is given.

4.1 CELLULOSE

The first sample investigated was pure cellulose, as described in section 2.1.1. All measurements were repeated at least two times to ensure reproducibility.

4.1.1 PALS

As already mentioned, the PALS measurements on all samples investigated were done according to the same sequence:

- Measurements on the “dry” sample (laboratory conditions (50 ± 2) % relative humidity): empty petri dish in measurement box (see figure 13)
- Measurements on the “wet” sample ((81 ± 2) % relative humidity):
  water filled petri dish in measurement box
- Measurements on the “dried” sample (< 10 % relative humidity):
  petri dish filled with silica gel in measurement box

In the following tables and figures, the blue shaded part of the graph includes the positron lifetime values which belong to the “wet” measurements, while the part of the graph including the measurements during drying are shaded in orange. The first measurement result, which corresponds to the time value 0, is always the result of the “dry” measurement.
In figure 18 the relative changes of the mean positron lifetime τ_{mean} in comparison to the mean lifetime corresponding to the “dry” sample state in dependence of time spent in humid

atmosphere are shown. In table 3 the corresponding absolute values of the mean positron lifetimes, the uncertainties, the three lifetime components τ_1, τ_2, τ_3 and corresponding intensities I_1, I_2, I_3 are shown.

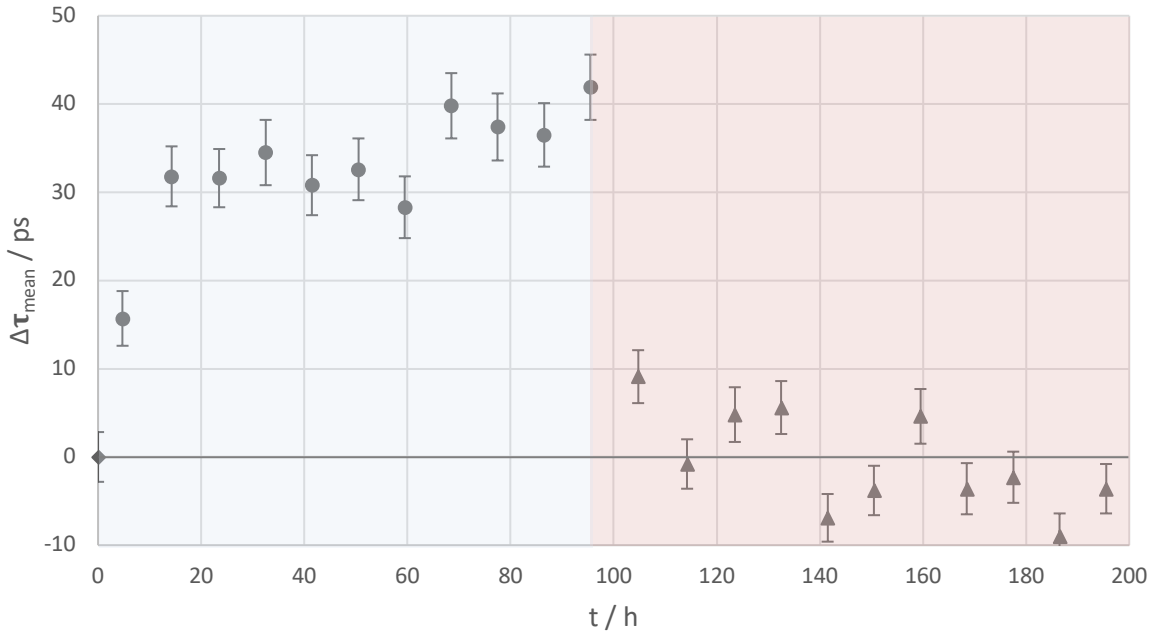

Figure 18: PALS measurement of cellulose: relative change in mean positron lifetime $\Delta\tau_{mean}$ in dependence of time *t* at a temperature of 20°C and a relative humidity of approximately 80% (blue shaded, dot-markers correspond to wet measurement), 10 % (orange shaded, triangle-markers correspond to dried measurement) and 50 % (diamond-marker correspond to dry measurement)

Table 3: PALS measurement of cellulose

t…time, τ_{mean}… mean positron lifetime, τ_i… positron lifetime component i, I_i… Intensity of lifetime component i

t / h	τ_{mean} / ns	τ_1 / ns	I_1 /ns	τ_2 / ns	I_2 / ns	τ_3 / ns	I_3 / ns
0	0,527	0,179	23,947	0,359	57,647	1,508	18,406
4,75	0,543	0,197	26,172	0,361	55,524	1,591	18,304
14,25	0,559	0,195	23,218	0,356	58,234	1,654	18,548
23,5	0,559	0,156	15,905	0,342	65,247	1,650	18,848
32,5	0,562	0,213	32,940	0,380	49,327	1,715	17,732
41,5	0,558	0,185	21,913	0,352	59,532	1,660	18,556
50,5	0,560	0,183	21,041	0,353	60,658	1,679	18,301
59,5	0,556	0,188	24,222	0,361	57,794	1,676	17,985
68,5	0,567	0,211	30,114	0,371	51,582	1,715	18,193
77,5	0,565	0,225	37,742	0,391	44,421	1,717	17,837
86,5	0,564	0,174	20,750	0,357	61,249	1,717	18,001
95,5	0,569	0,217	33,050	0,380	48,918	1,729	18,032
104,75	0,537	0,175	22,388	0,357	59,466	1,571	18,146
114,25	0,527	0,162	18,986	0,347	61,842	1,467	19,172
123,5	0,532	0,189	29,291	0,385	52,803	1,528	17,906
132,5	0,533	0,190	28,282	0,377	53,355	1,514	18,363
141,5	0,521	0,189	25,313	0,354	54,678	1,396	20,010
150,5	0,524	0,173	22,010	0,355	58,767	1,440	19,224
159,5	0,532	0,203	34,508	0,395	47,418	1,519	18,074
168,5	0,524	0,205	33,799	0,387	47,457	1,444	18,744
177,5	0,525	0,180	26,065	0,373	55,819	1,492	18,116
186,5	0,518	0,156	20,158	0,349	60,014	1,394	19,828
195,5	0,524	0,192	30,876	0,383	50,680	1,466	18,444

Figure 18 shows that the mean positron lifetime increases with increasing time spent in humid atmosphere. After approximately 20 hours the increase of the mean positron lifetime τ_{mean} slows down. About 70 hours after placing the sample in the wet surrounding there is a second increase in the mean positron lifetime τ_{mean}. Once drying the air with silica gel, to a relative humidity of less than 10 %, the mean positron lifetime decreases rapidly, after approximately 10 hours the mean positron lifetime does not change significantly anymore. The measurement results show that, when drying the sample, the mean positron lifetime $\tau_{mean,dried}$ reaches the value of the mean positron lifetime before moistening the sample, in the dry state τ_{dry}.

In table 3, besides the mean positron lifetime τ_{mean}, also the lifetime components with corresponding uncertainties and intensities are shown. The lifetime components τ_1, which is approximately 0.2 ns and probably belongs to the p-Ps component, which is 0.125 ns in vacuum (see section 1.4), and τ_2, which is between 0.3 ns and 0.4 ns, do not exhibit a trend, but the longest lifetime component τ_3 does. It increases with time in a wet environment and decreases when the cellulose is dried. The lifetime component τ_3 has a value of 1.5 ns, when the cellulose absorbs water in the wet surrounding it increases up to 1.7 ns and decreases

again while drying to approximately 1.4 ns. That means, τ_3 is mainly responsible for the appropriate change in the mean positron lifetime. This long lifetime component could correspond to the positron annihilation in the water of the cellulose. Earlier measurements on positron lifetimes in water also showed one long lifetime component of approximately 1.8 ns at 20°C [54,55]. Another possibility is that this component corresponds to the ortho-Ps component which increases with higher water content due to the higher volume of the pores. Recent works of PALS with pure, dry cellulose suggest that the long lifetime component is o-Ps formation in the pores of the cellulose. The intermediate lifetime component τ_2, which also between 0.3 and 0.4 ns in recent investigations [5] is not well understood yet. There are two possible explanation for the value of this component: whether it is fast pick-off-process of o-Ps in regions with high electron density and therefore high cristallinity or it results from free positrons which annihilate in the bulk. In general, do the measurement lifetime components and intensities correspond very well to former PALS measurements in cellulose [5].

4.1.2 CONTACT ANGLE MEASUREMENT

Contact angle measurements give information about the wettability of a material. It is difficult to investigate pure cellulose with this method, because cellulose is a very hydrophilic material. The figures 19 represents an image of the high-resolution camera in the measurement set-up. It can be seen that the contact angle of cellulose is much smaller than 10°, which means that cellulose is a so-called super-hydrophilic material.

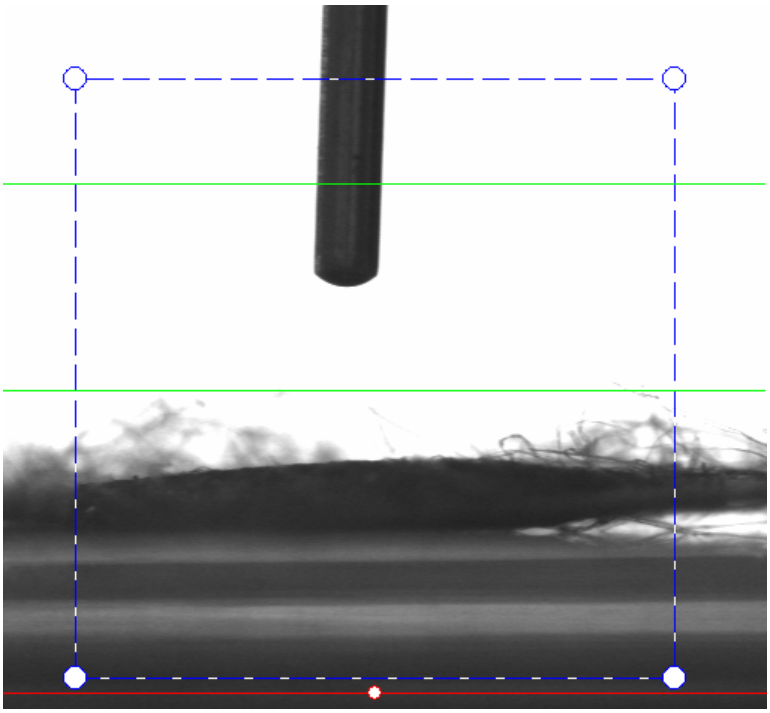

Figure 19: Example of a contact angle measurement on cellulose: The space between the green lines mark the droplet's size, the grey surface on the bottom is the cellulose sample. The droplet disappears immediately when it is placed on the cellulose.

4.1.3 WATER CONTENT

The water content of the cellulose increases with high relative humidity of the environment in the measurement box and decreases with lower relative humidity. All measurements show a saturation of the water intake after about four hours with high humidity. Drying with silica gel takes place even faster, after two to three hours the mass does not change significantly anymore. This can be seen in figure 20. It is remarkable, that the process of water absorption takes place much faster than the change in the mean positron lifetime $\Delta\tau_{mean}$.

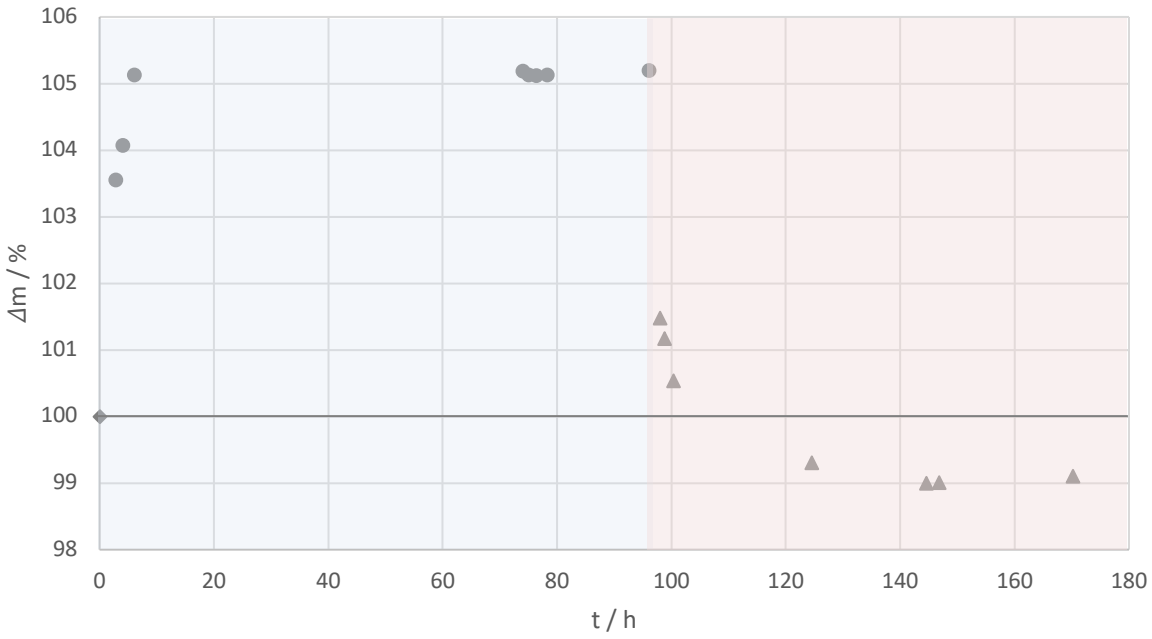

Figure 20: Water content measurement of cellulose: relative mass change Δm in dependence of time t at a temperature of 20°C and a relative humidity of approximately 80 % (blue shaded, dot-markers correspond to wet measurement), 10 % (orange shaded, triangle-markers correspond to dried measurement) and 50 % (diamond-marker correspond to dry measurement)

The relative mass change Δm is calculated according to

$$\Delta \mathrm{m} = \frac{\mathrm{m_{ges,i} - m_W}}{\mathrm{m_{ges,0} - m_W}} \tag{21}$$

where $m_{ges,i}$ is the weighted mass, that means the sample plus the wire which holds sample and source together (there is no radioactive source included in the case of the water content measurement but the sample is prepared the same way as for the PALS measurement). Here,

m_W is the mass of the wire and $m_{ges,0}$ is the weighted mass of the dry sample at t = 0 h, including the mass of the wire.

The uncertainty of the relative mass change $\sigma_{\Delta m}$ was calculated with the method of the largest error, for the water content, that means, that the uncertainty for each value is calculated by

$$\sigma_{\Delta m} = \left|\frac{1}{m_{ges,0}-m_W}\right| \sigma_m + \left|\frac{m_{ges,i}-m_{ges,0}}{(m_{ges,0}-m_W)^2}\right| \sigma_m + \left|\frac{m_W-m_{ges,i}}{(m_{ges,0}-m_W)^2}\right| \sigma_m \qquad (22)$$

where σ_m denotes the uncertainty of the scale. The uncertainty of the scale is assumed to be $\sigma_m = 0.01\ \mathrm{mg}$, actually the scale has a nominal precision of $0.001\ \mathrm{mg}$ but due to different relative humidity in the box and the scale, the mass changes rapidly and an exact scaling with respect to the last digit of the scale is not possible.

4.1.4 PALS AND WATER CONTENT

For reasons of comparison, figure 21 shows the PALS and water content measurements of the cellulose sample in one diagram. It can be seen that the increase in mean positron lifetime $\Delta\tau_{mean}$ takes place on a longer time scale compared to the change of the water content Δm. This will be discussed in more detail in section 4.4.1. In case of PALS measurements, a sufficient number of annihilation processes is necessary to ensure good statistics. Hence, it takes about eight to ten hours of measurement time to generate a statistically meaningful mean positron lifetime value. The time resolution of the water content measurements is much lower, usually it is an hour. Due to this, there is a time delay between the change in mean positron lifetime τ_{mean} and the change in relative mass Δm. This can be seen best in the first hours after placing the sample in a humid environment (0 – 20 h in figure 26). The same holds on when placing the sample in a dry atmosphere (140 – 150 h in figure 26).

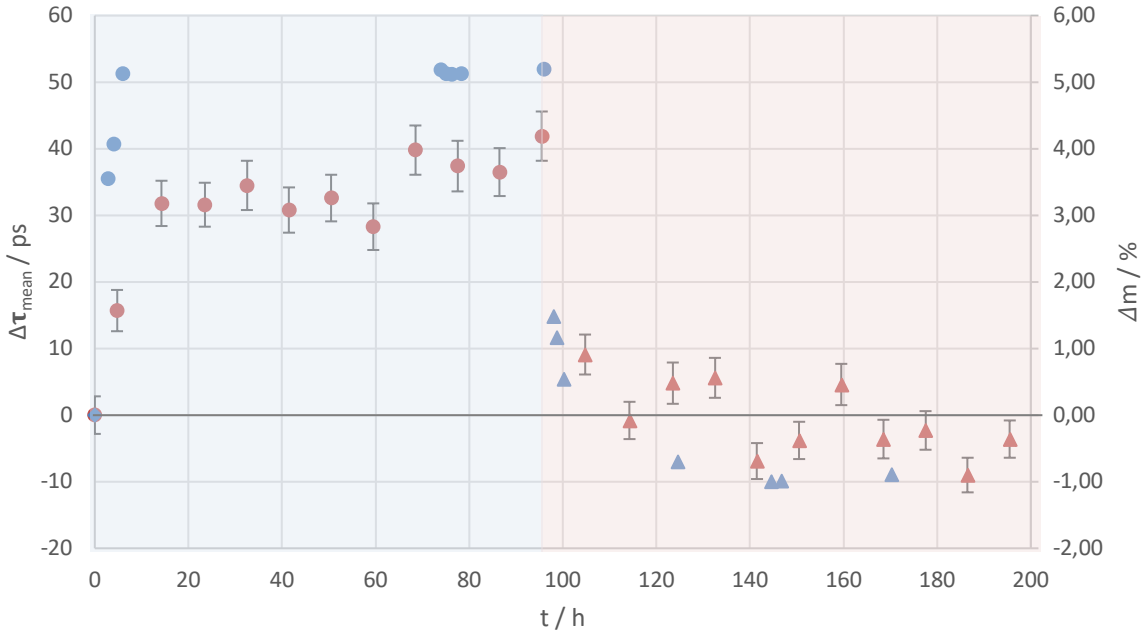

Figure 21: Water content and PALS measurement of cellulose: relative mass change Δm and change of the mean positron lifetime $\Delta\tau_{mean}$ in dependence of time t at a temperature of 20°C and a relative humidity of approximately 80% (blue shaded, dot-markers correspond to wet measurement), 10 % (orange shaded, triangle-markers correspond to dried measurement) and 50 % (diamond-marker correspond to dry measurement)

4.2 FINE PAPER

Besides cellulose also fine paper was investigated by PALS, contact angle measurements and monitoring the water content applying the same measurement procedure (dry sample – wet sample – dried sample for the case of PALS measurement). The main difference to cellulose is that fine paper does not only consist of cellulose but also of hemicellulose and other filling material (see section 2.1). This leads to a slightly different behavior in water absorption and the evolution of the mean positron lifetime.

4.2.1 PALS

Figure 22 and table 4 show the results of the PALS measurement of fine paper. Here also, the part of the graph including the positron lifetime values measured in the "wet" state of the sample is shaded in blue and the part of the graph including the positron lifetimes during drying is shaded orange. The change of the mean positron lifetime $\Delta\tau_{mean}$ due to water intake reaches a maximum value of 25 ps after approximately 50 h. When drying the fine paper sample again, also the mean positron lifetime decreases to the range of the original (= "dry") value. Compared to cellulose, the maximum change measured of the mean positron lifetime $\Delta\tau$ is about 40 % smaller.

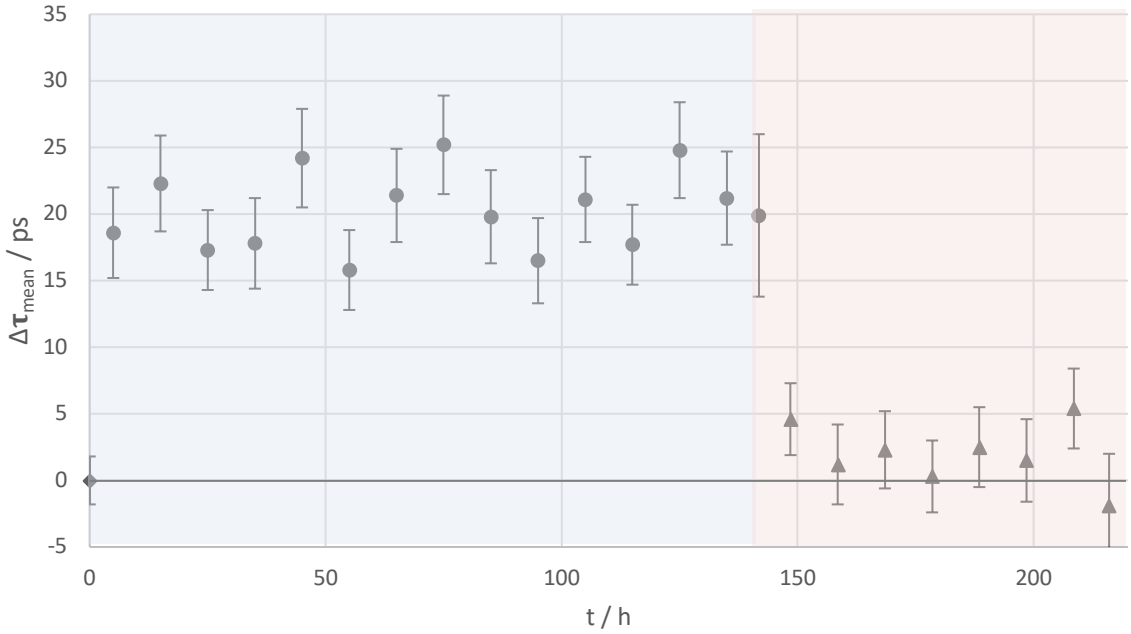

Figure 22: PALS measurement of fine paper: relative change in mean positron lifetime $\Delta\tau_{mean}$ in dependence of time t at a temperature of 20°C and a relative humidity of approximately 80 % (blue shaded, dot-markers correspond to wet measurement), 10 % (orange shaded, triangle-markers correspond to dried measurement) and 50 % (diamond-marker correspond to dry measurement)

Table 4: PALS measurement of fine paper
t... time, τ_{mean}... mean positron lifetime, τ_i... positron lifetime component i, I_i... Intensity of lifetime component i

t / h	τ_{mean} / ns	τ_1 / ns	I_1 /ns	τ_2 / ns	I_2 / ns	τ_3 / ns	I_3 / ns
0	0,451	0,224	39,909	0,374	48,213	1,530	11,878
5	0,470	0,223	41,226	0,384	47,203	1,705	11,542
15	0,474	0,223	42,435	0,392	46,196	1,741	11,370
25	0,469	0,195	20,120	0,334	67,112	1,604	12,769
35	0,469	0,229	42,670	0,383	45,615	1,677	11,715
45	0,475	0,247	54,597	0,413	33,773	1,731	11,630
55	0,467	0,206	26,441	0,343	60,693	1,588	12,867
65	0,473	0,236	44,680	0,383	43,532	1,703	11,788
75	0,476	0,234	46,270	0,395	42,313	1,760	11,417
85	0,471	0,226	41,098	0,380	47,258	1,706	11,645
95	0,468	0,224	36,291	0,360	51,367	1,634	12,342
105	0,472	0,214	31,547	0,355	55,931	1,648	12,522
115	0,469	0,189	19,795	0,333	67,462	1,622	12,743
125	0,476	0,222	38,958	0,375	49,453	1,762	11,589
135	0,472	0,240	47,286	0,387	40,766	1,683	11,948
141,75	0,471	0,252	56,608	0,406	31,056	1,639	12,336
148,5	0,456	0,231	32,190	0,347	54,168	1,417	13,642
158,5	0,452	0,224	39,225	0,381	49,118	1,522	11,657
168,5	0,454	0,246	50,624	0,398	36,894	1,459	12,482
178,5	0,452	0,224	32,732	0,353	53,847	1,403	13,421
188,5	0,454	0,249	53,497	0,408	34,313	1,480	12,190
198,5	0,453	0,242	49,698	0,403	38,480	1,499	11,822
208,5	0,457	0,239	46,916	0,396	40,938	1,502	12,147
216	0,449	0,237	43,514	0,372	43,456	1,417	13,030

4.2.2 CONTACT ANGLE MEASUREMENT

The contact angle measurements with fine paper are shown in figure 23 and 24. Due to the very fast water intake of fine paper, the droplet shrinks in a few seconds and an exact determination of the angle is not possible. Compared to the contact angle measurement on the cellulose sample (figure 19), the angle is bigger but after approximately 10 seconds (figure 24), the droplet is not cognizable anymore because the water is completely absorbed by the paper and the paper corrugates.

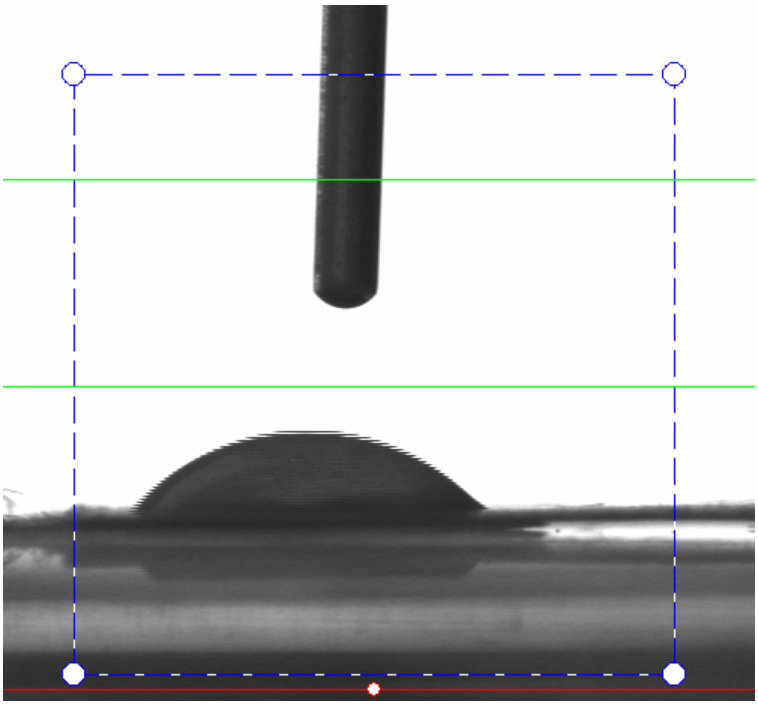

Figure 23: Contact angle measurement on fine paper, 2 seconds after placing the droplet. The space between the green lines mark the droplet's size, the grey surface on the bottom is the fine paper sample. The droplet disappears a few seconds after placing it on the fine paper.

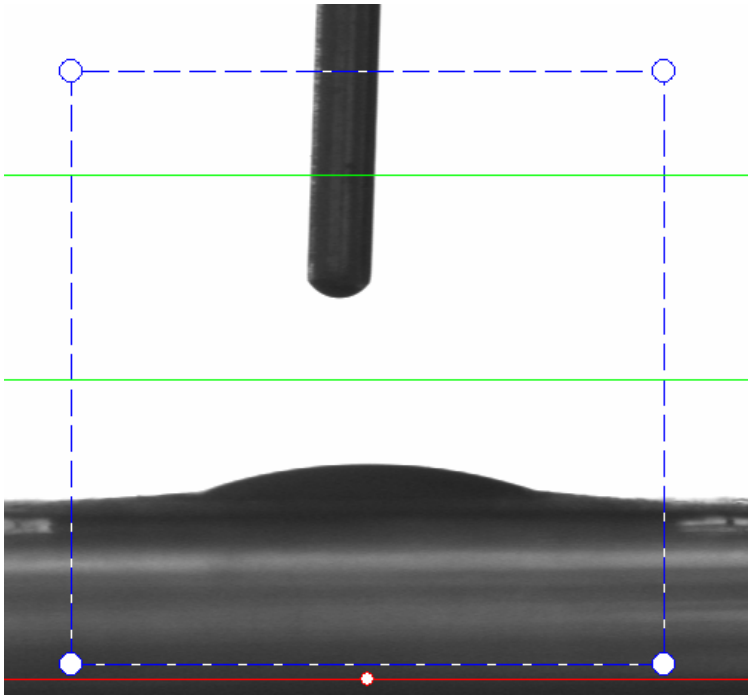

Figure 24: Contact angle measurement on fine paper, 10 seconds after placing the droplet. The space between the green lines mark the droplet's size, the grey surface on the bottom is the fine paper sample. The droplet disappears a few seconds after placing it on the fine paper.

4.2.3 WATER CONTENT

The water intake of the fine paper sample is similar to cellulose. It takes place on the same time scale but the relative mass change is about 3% lower, this suggests that fine paper takes in less water than cellulose which could explain the smaller change of the mean positron lifetime τ_{mean} for fine paper. Figure 25 shows the results of the water content measurements for fine paper.

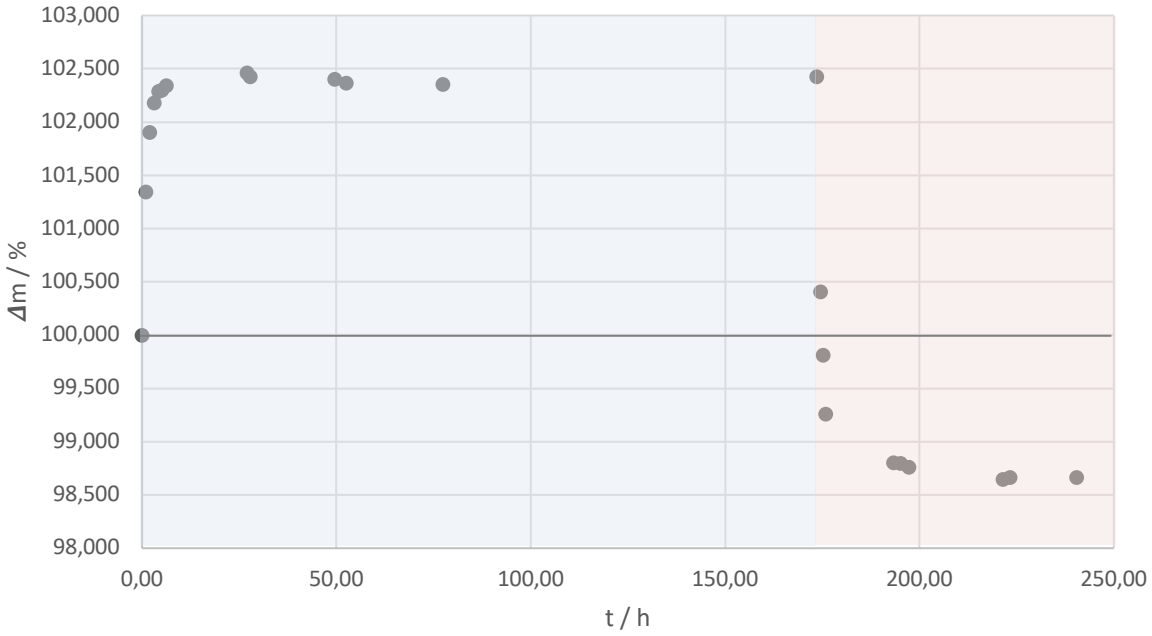

Figure 25: Water content measurement of fine paper: relative mass change *Δm* in dependence of time *t* at a temperature of 20°C and a relative humidity of approximately 80 % (blue shaded, dot-markers correspond to wet measurement), 10 % (orange shaded, triangle-markers correspond to dried measurement) and 50 % (diamond-marker correspond to dry measurement)

4.2.4 PALS AND WATER CONTENT

Figure 26 shows the PALS and water content measurements of the fine paper sample in one diagram. Like for cellulose, also here the increase in mean positron lifetime $\Delta\tau_{mean}$ takes place on a longer time scale compared to the change of the water content Δm.

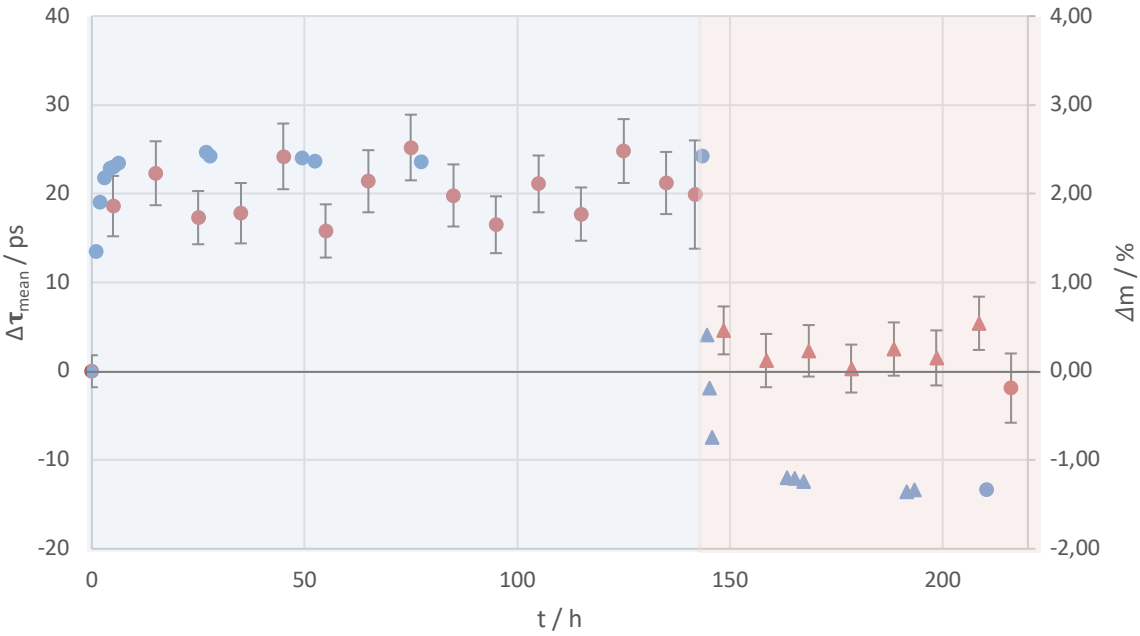

Figure 26: Water content and PALS measurement of fine paper: relative mass change Δm and change of the mean positron lifetime $\Delta\tau_{mean}$ in dependence of time t at a temperature of 20°C and a relative humidity of approximately 80 % (blue shaded, dot-markers correspond to wet measurement), 10 % (orange shaded, triangle-markers correspond to dried measurement) and 50 % (diamond-marker correspond to dry measurement)

4.3 KRAFT SACK PAPER

The big difference between fine paper, cellulose and Kraft sack paper is, that Kraft sack paper contains lignin. This does not only lead to the brown color, compared to the white one of cellulose and fine paper, but also to a different behavior when it comes to water intake because lignin is a hydrophobic substance. As will be shown in the following, especially the PALS measurement shows a different behavior for Kraft sack paper than for fine paper and pure cellulose.

4.3.1 PALS

In figure 27 and table 5 the results of the PALS measurement for Kraft sack paper are shown. Compared to the other materials investigated, one can see two distinct plateaus instead of one. The first one occurring after approximately 20 hours and the second one setting in after at approximately 70 hours. This measurement was repeated three times in total and in all these measurements those two plateaus were observed. The total maximum change in the mean positron lifetime $\Delta\tau_{mean}$ is smaller than for cellulose but higher than for fine paper. A reason for this could be the water intake, but this will be discussed in section 3.3.3.

As can be seen in table 5, the second lifetime component τ_3 increases with the time spent in the wet surrounding and decreases in the dry one, as already observed for the other two cellulose materials. The other two lifetime components do not follow a trend.

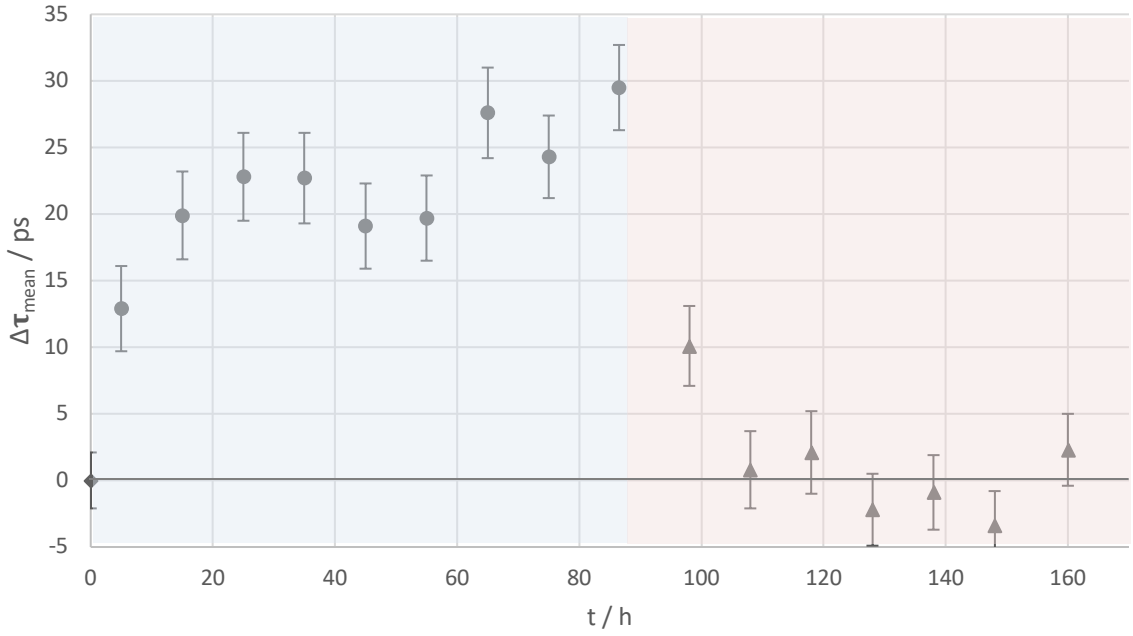

Figure 27: PALS measurement of Kraft sack paper: relative change in mean positron lifetime $\Delta\tau_{mean}$ in dependence of time *t* at a temperature of 20°C and a relative humidity of approximately 80 % (blue shaded, dot-markers correspond to wet measurement), 10 % (orange shaded, triangle-markers correspond to dried measurement) and 50 % (triangle-marker correspond to dry measurement)

Table 5: PALS measurement of Kraft sack paper
t... time, τ_{mean}... mean positron lifetime, τ_i... positron lifetime component i, I_i... Intensity of lifetime component i

t / h	τ_{mean} / ns	τ_1 / ns	I_1 /ns	τ_2 / ns	I_2 / ns	τ_3 / ns	I_3 / ns
0	0,475	0,226	39,478	0,395	47,583	1,531	12,939
5	0,488	0,193	19,374	0,350	67,282	1,614	13,344
15	0,495	0,233	36,258	0,376	49,854	1,606	13,889
25	0,498	0,205	24,002	0,357	62,396	1,662	13,603
35	0,498	0,225	35,624	0,376	50,747	1,664	13,630
45	0,494	0,206	22,584	0,353	63,683	1,625	13,733
55	0,495	0,198	20,200	0,349	65,973	1,624	13,827
65	0,503	0,209	23,556	0,353	62,556	1,675	13,888
75	0,499	0,192	18,734	0,346	66,888	1,614	14,378
86,5	0,505	0,234	38,272	0,384	48,086	1,689	13,641
98	0,485	0,190	20,521	0,350	65,600	1,559	13,879
108	0,476	0,225	38,377	0,386	47,858	1,486	13,766
118	0,477	0,231	41,273	0,400	45,899	1,546	12,828
128	0,473	0,181	21,000	0,353	65,132	1,477	13,868
138	0,474	0,208	27,330	0,359	58,576	1,468	14,094
148	0,472	0,204	23,894	0,347	61,184	1,411	14,922
160	0,477	0,230	39,905	0,392	47,047	1,542	13,048

4.3.2 CONTACT ANGLE MEASUREMENT

Figures 28 to 32 show the contact angle measurements of Kraft sack paper. Compared to the other materials, Kraft sack paper is hydrophobic due to its high lignin content. For that reason, the contact angle measurements are more meaningful than the previous, because a droplet on the Kraft sack paper keeps its shape for a long time and does not melt away in the blink of an eye like for cellulose and fine paper.

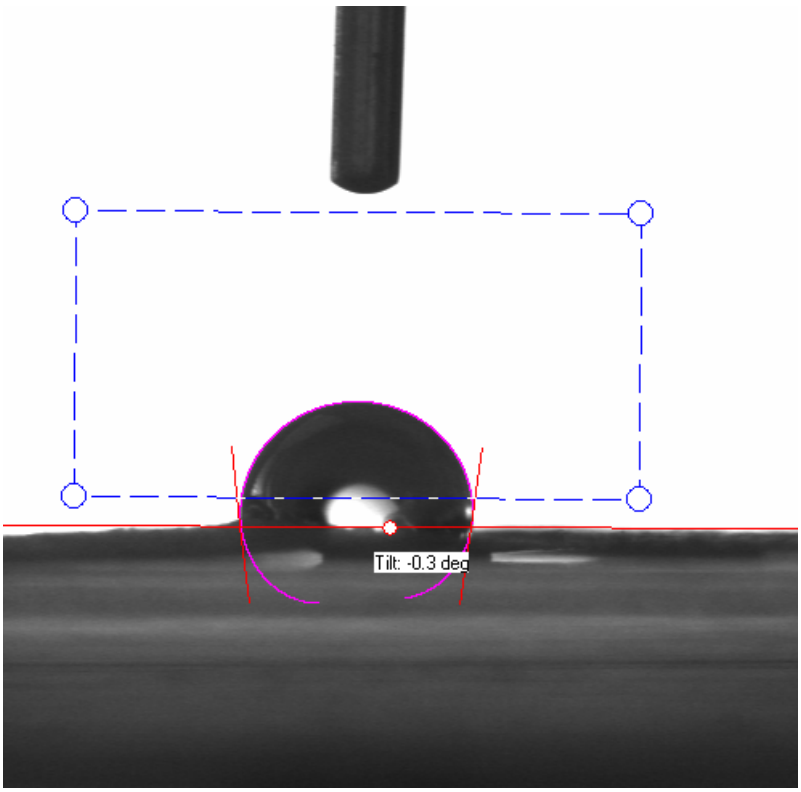

Figure 28: Contact angle measurement on Kraft sack paper 1/5: The space between the green lines mark the droplet's size, the grey surface on the bottom is the Kraft sack paper sample. The droplet does not deliquesce.

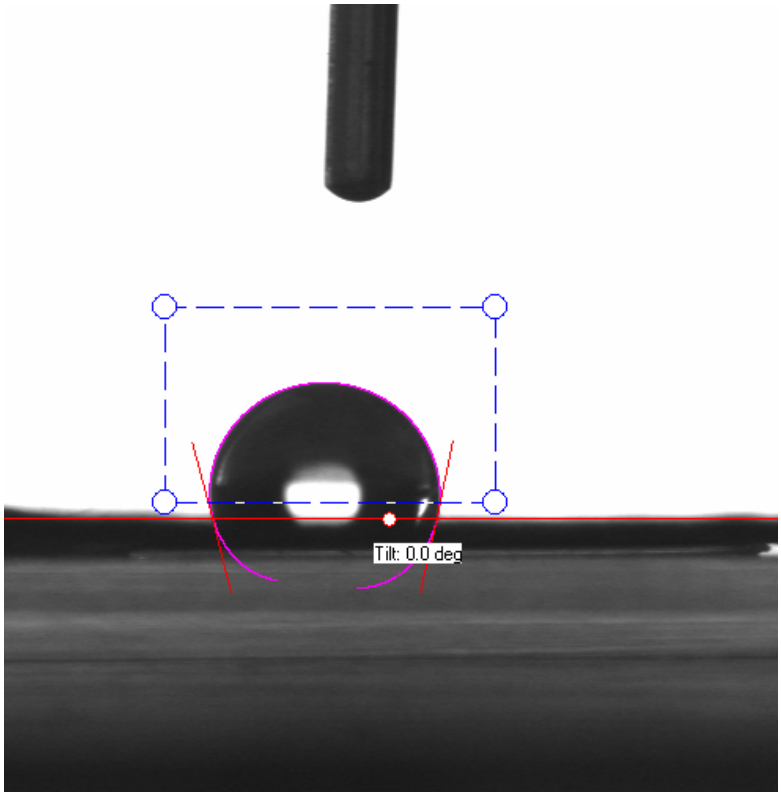

Figure 29: Contact angle measurement on Kraft sack paper 2/5: The space between the green lines mark the droplet's size, the grey surface on the bottom is the Kraft sack paper sample. The droplet does not deliquesce.

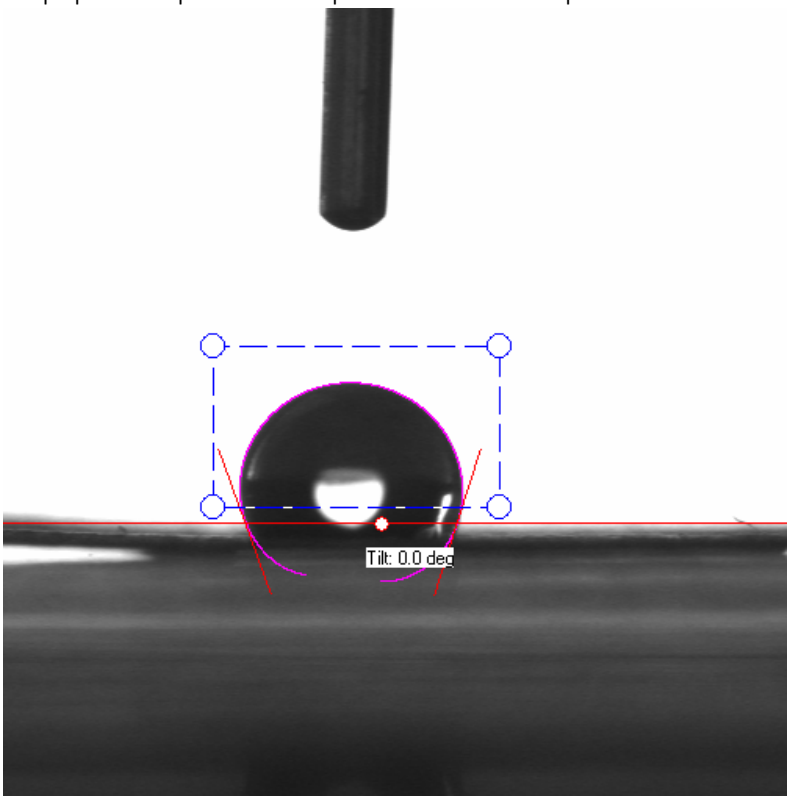

Figure 30: Contact angle measurement on Kraft sack paper 3/5: The space between the green lines mark the droplet's size, the grey surface on the bottom is the Kraft sack paper sample. The droplet does not deliquesce.

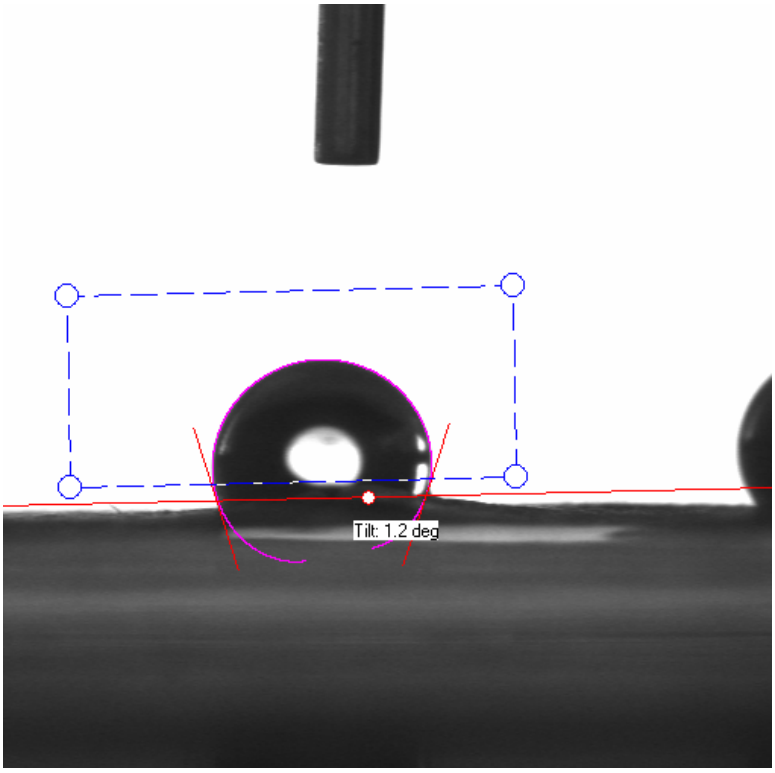

Figure 31: Contact angle measurement on Kraft sack paper 4/5: The space between the green lines mark the droplet's size, the grey surface on the bottom is the Kraft sack paper sample. The droplet does not deliquesce.

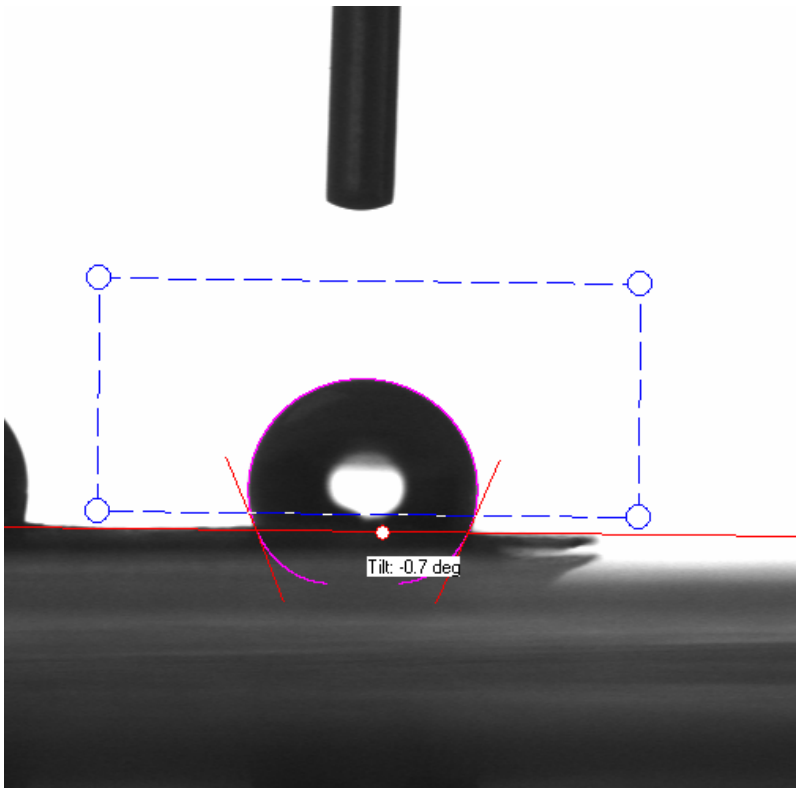

Figure 32: Contact angle measurement on Kraft sack paper 5/5: The space between the green lines mark the droplet's size, the grey surface on the bottom is the Kraft sack paper sample. The droplet does not deliquesce.

Table 8 shows the measured angles from figures 18 to 32. All angles are bigger than 90°, that means Kraft sack paper is hydrophobic. Due to the different influences on the measurement, like evenness of the paper, impurities on the surface or the unregular structure of paper materials in general, contact angle measurements on paper materials have typically a variation in the results up to 20 %. The measurements in table 6 show a variation in the contact angles of less than ± 10 %, which suggests a meaningful result.

Table 6: Contact angles of Kraft sack paper

θ_l... left angle

θ_r... right angle

Number	θ_l	θ_r
1	96.5	97.9
2	104.1	102.3
3	109.8	107.7
4	106.2	109.3
5	112.9	113.2

The mean of the contact angles is according to table 6

$$\theta = (106 \pm 6)°.$$

4.3.3 WATER CONTENT

Figure 33 shows the relative mass change Δm of Kraft sack paper due to moisture intake. As can be seen in figure 33, the water intake is saturated after a few hours, similar to cellulose and fine paper.

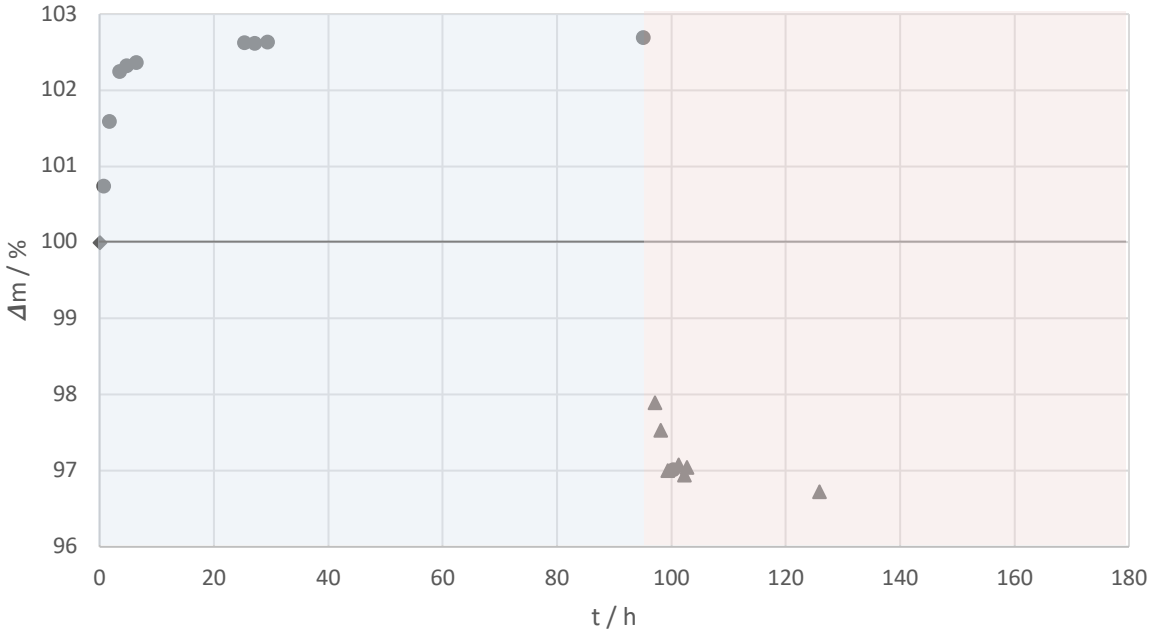

Figure 33: Water content measurement of Kraft sack paper: relative mass change Δm in dependence of time t at a temperature of 20°C and a relative humidity of approximately 80 % (blue shaded, dot-markers correspond to wet measurement), 10 % (orange shaded, triangle-markers correspond to dried measurement) and 50 % (diamond-marker correspond to dry measurement)

Compared to the other cellulose materials, the relative mass change Δm is similar to fine paper and therefore lower than for pure cellulose. It is remarkable, that the mass relative to the original “dry” (laboratory conditions) mass when drying the sample with silica gel decreases to only 97 %. In comparison, fine paper and cellulose decrease to 99 %, when comparing the “dry” and “dried” mass.

4.3.4 PALS AND WATER CONTENT

Figure 34 shows the PALS and water content measurements of the Kraft sack paper sample in one diagram. Again, the increase in mean positron lifetime $\Delta\tau_{mean}$ takes place on a longer time scale compared to the change of the water content Δm.

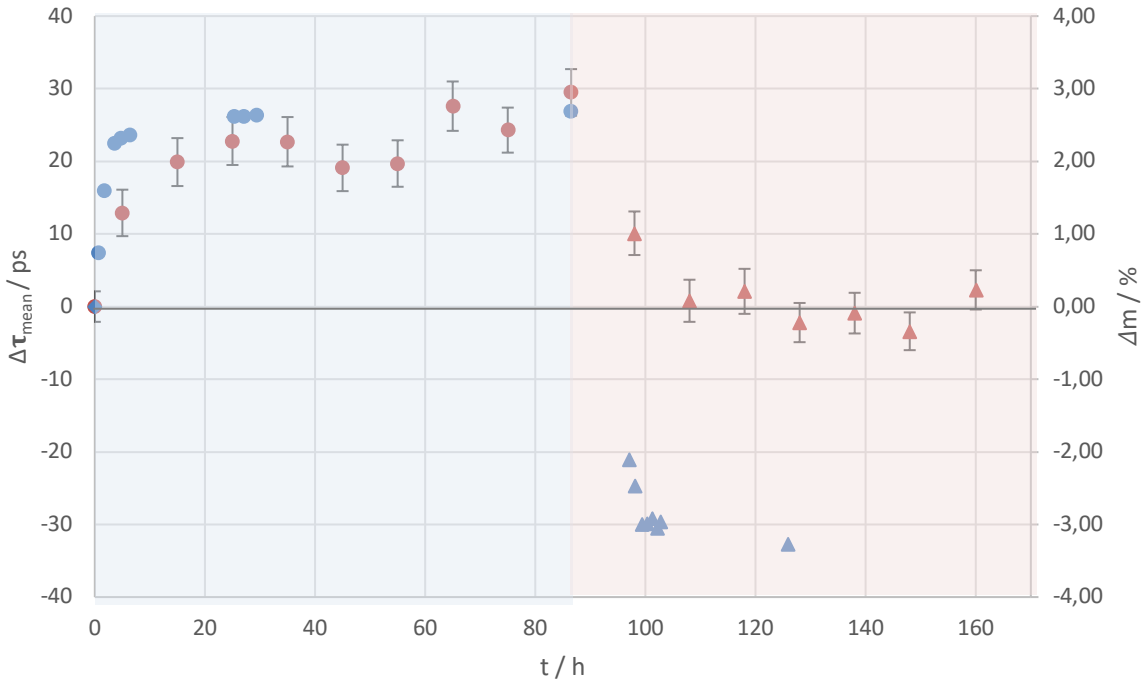

Figure 34: Water content and PALS measurement of Kraft sack paper: relative mass change Δm and change of the mean positron lifetime $\Delta\tau_{mean}$ in dependence of time t at a temperature of 20°C and a relative humidity of approximately 80 % (blue shaded, dot-markers correspond to wet measurement), 10 % (orange shaded, triangle-markers correspond to dried measurement) and 50 % (diamond-marker correspond to dry measurement)

4.4 COMPARISON OF THE RESULTS

In this section, the PALS and water content measurements of the three different materials investigated are represented and superimposed in one diagram, for reasons of comparison. The results of the contact angle measurements of each material are also summarized in one table. Due to the different lignin content of the three materials different behaviour in water sorption are expected.

4.4.1 PALS AND WATER CONTENT

In figure 35 the PALS measurement for cellulose (orange dots), fine paper (blue dots) and Kraft sack paper (green dots) in the "wet" environment are shown. One can see that cellulose has the highest relative change in the mean positron lifetime $\Delta\tau_{mean}$ compared to the dry sample of approximately 40 ps. For fine paper and Kraft sack paper the maximum change in mean positron lifetime $\Delta\tau_{mean}$ is between 25 ps and 30 ps, with respect to a measurement time of 100 hours.

To compare these results to the water intake of each material, figure 36 shows the relative mass change Δm due to water intake when the samples are placed in a surrounding of 80 % relative humidity. It can be seen that for all samples the water intake saturates after a few hours (< 5 h). The biggest change in relative mass occurs for cellulose, with more than 5 % increase. Fine paper and Kraft sack paper have a maximum change in mass Δm of less than half compared to the value for cellulose.

These results suggest that more water intake leads to a higher change in mean positron lifetime. Possible explanations for that are, that water has a long positron lifetime component of approximately 1.8 ns [54,55] and positron annihilation within water increases the mean positron lifetime with increasing water content of the sample. Another explanation is that the pores widen with increased water content and the o-Ps formation in this open volume increases.

It is also remarkable, that the water intake as well as the maximum mean positron lifetime τ_{mean} is slightly higher for Kraft sack paper than for fine paper. Kraft sack paper contains hydrophobic lignin which would suggest that it would absorb less water than fine paper.

If one assumes that the pore size of cellulose materials does not change anymore after the water intake took place, i.e., after a few hours, the question arises why the mean positron lifetime τ_{mean} continuously varies for times significantly longer than that. A possible explanation could be that sorption processes from the material surface occur on a longer time scale.

While for fine paper the relative change of the mean positron lifetime $\Delta\tau_{mean}$ seems to stay more or less constant at a value $\Delta\tau \approx$ 20 ps already after 10 - 20 hours, the mean positron lifetime of cellulose and Kraft sack paper shows a second increase of $\Delta\tau \approx$ 5-10 ps after 60 - 70 hours in humid atmosphere. This leads to two plateaus in the lifetime curve of cellulose and Kraft sack paper, one between 20 hours and 60 hours and the other one between 60 hours and 100 hours. These results are especially interesting when looking at the water content in figure 36 because the water content stays constant in these time spans. A possible reason for the second plateau in the Kraft sack paper could be that the surface sorption processes of the water into the material take place at different time scales. Because the aromatic groups in the lignin are hydrophobic while the keto groups are hydrophilic. This could lead to two different time scales of surface ab- and adsorption, depending on where the water molecules are docking on the surface of the Kraft sack paper. Something similar holds for cellulose, when a water molecule is localized at a hydrophilic carboxyl or hydroxyl group on the surface it is ab- and adsorbed faster than on other surface areas which are not hydrophilic. That means, that the location of the water molecule on the surface of the sample has an influence on the time the mean positron lifetime τ_{mean} changes. Former studies reported that moisture intake in cellulose occurs at higher relative humidity (approximately 80 %) faster around carboxyl groups than around hydroxyl groups. While for lower relative humidity the moisture intake occurs in a more uniform manner [3].

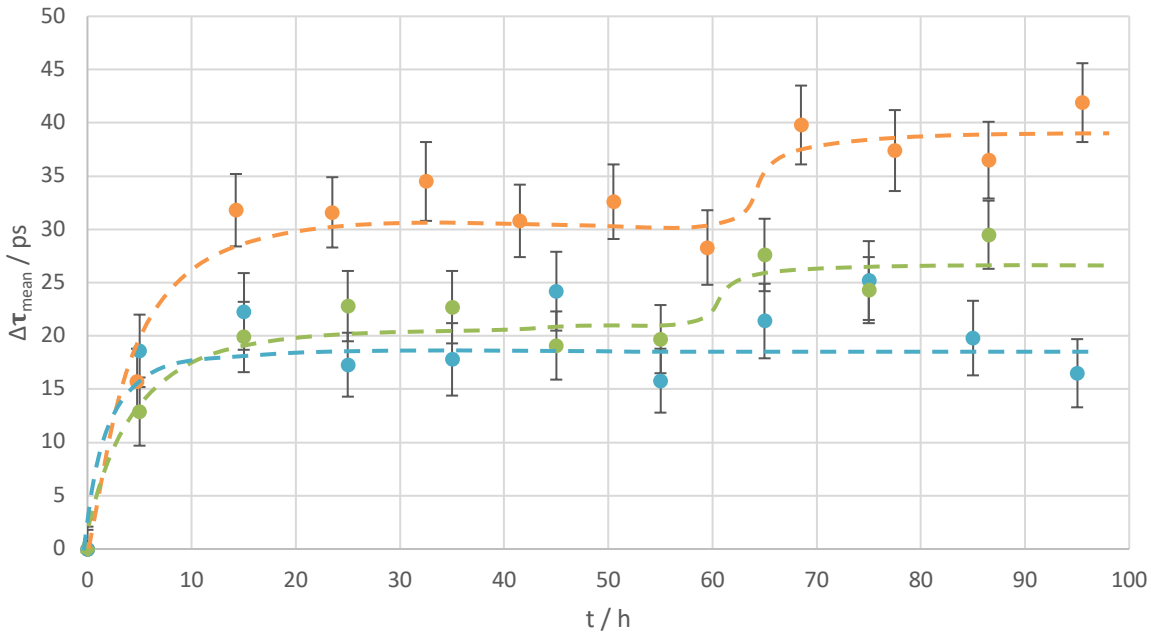

Figure 35: PALS "wet" measurement of cellulose (orange), fine paper (blue) and Kraft sack paper (green): relative change in mean positron lifetime $\Delta\tau_{mean}$ in dependence of time t at a temperature of 20°C and a relative humidity of approximately 80 % (dot-markers correspond to wet measurement) and 50 % (diamond - marker correspond to dry measurement). (Lines are drawn for guiding the eyes).

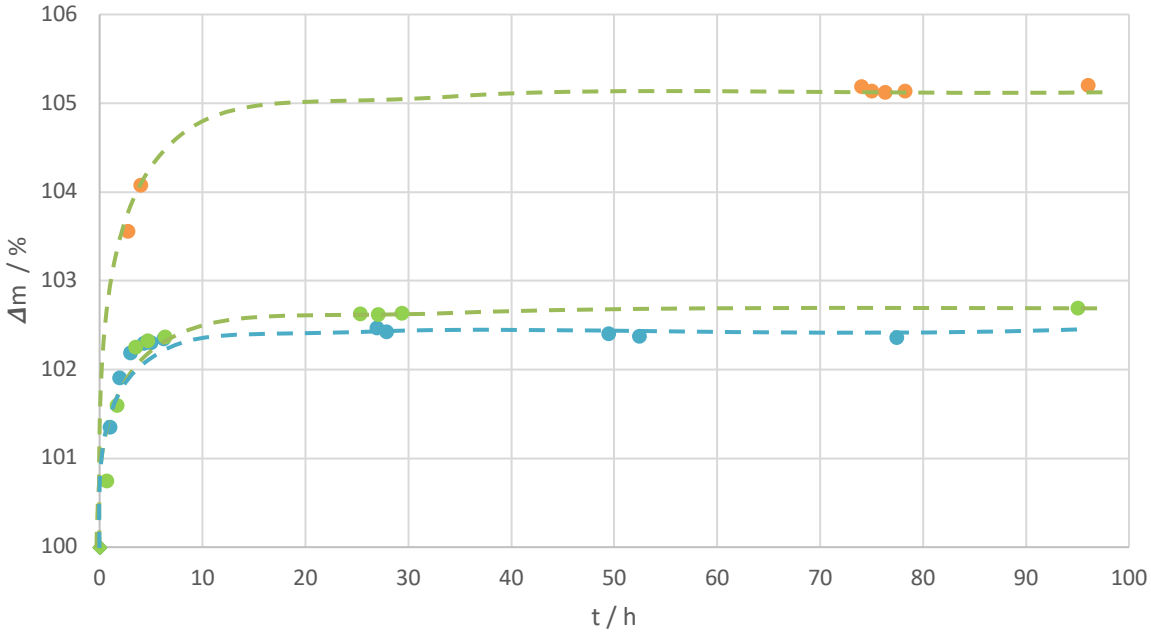

Figure 36: Water content "wet" measurement of cellulose (orange), fine paper (blue) and Kraft sack paper (green): relative mass change Δm in dependence of time t at a temperature of 20°C and a relative humidity of approximately 80 % (dot-markers correspond to wet measurement) and 50 % (diamond-marker correspond to dry measurement). (Lines are drawn for guiding the eyes).

For a further comparison of Kraft sack paper, fine paper and cellulose also the PALS measurements in the "dried" surrounding with silica gel will be compared for all samples.
The change in the mean positron lifetime $\Delta\tau_{mean}$ is shown in figure 37 for cellulose, fine paper and Kraft sack paper depending on time in "dried" atmosphere (silica gel in petri dish decreases the relative humidity to approximately 10 % in the measurement box). The value at time 0 in figure 37 corresponds to the mean positron lifetime after moistening the sample. The "dry" value, before moistening, correspond to $\Delta\tau_{mean}$ = 0 ps in figure 37.
Although the change in the mean positron lifetime $\Delta\tau_{mean}$ for cellulose is more than double of the mean positron lifetime change $\Delta\tau_{mean}$ of fine paper after placing it in a "wet" surrounding, after approximately 20 hours all three samples show the initial ("dry", value 0 in figure 36) mean positron lifetime. From this time on the values scatter around the positron lifetime value for the "dry" sample and do not change significantly anymore. This is especially noticeable because it is well known in paper physics that paper swells when it dries. According to this, drying causes an irreversible contraction of the fiber cell wall. This leads to a lower extent of the cellulose fiber after drying [1]. The results of this thesis do not make any statement of the fiber cell walls but only on the amount and size of pores and these seem to be about the same size before moistening and after drying.

Figure 38 shows the corresponding relative mass change Δm due to change in water content in dependence of time in "dried" atmosphere. The water content measurements show that the drying takes place as fast as the moistening, or even slightly faster. After a few hours the masses of all three samples do not change significantly anymore, although cellulose has taken up more than double of the water amount relative to its mass compared with the two paper samples. It is noticeable that Kraft sack paper seems to include the least amount of water compared to its initial ("dry", value 100 % in figure 40) mass, down to 97 %, while cellulose and fine paper stagnate around 99 % of their "dry" masses. This would suggest that Kraft sack paper has the highest amount of water at "dry" conditions (50 % relative humidity) or that there is a different kind of binding of the water in the material.

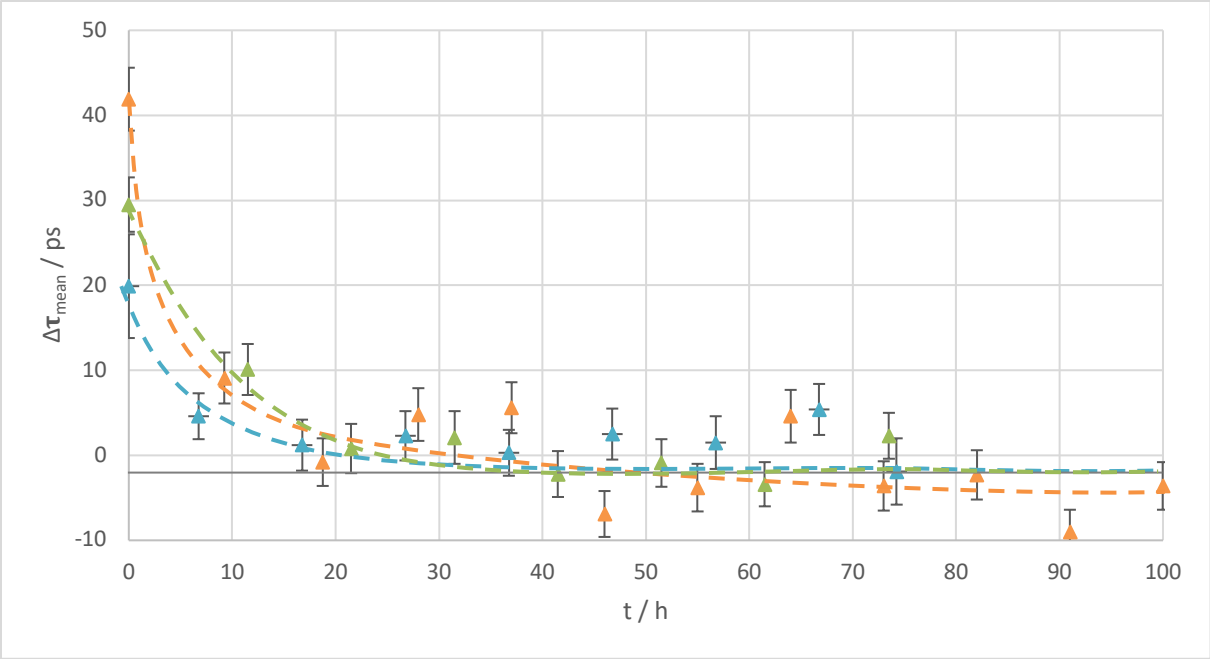

Figure 37: PALS "dried" measurement of cellulose (orange), fine paper (blue) and Kraft sack paper (green) : relative change in mean positron lifetime $\Delta\tau_{mean}$ in dependence of time *t* at a temperature of 20°C and a relative humidity of approximately 10 % (triangle-markers correspond to dried measurement) and 80 % (dot-marker correspond to dry measurement). (Lines are drawn for guiding the eyes).

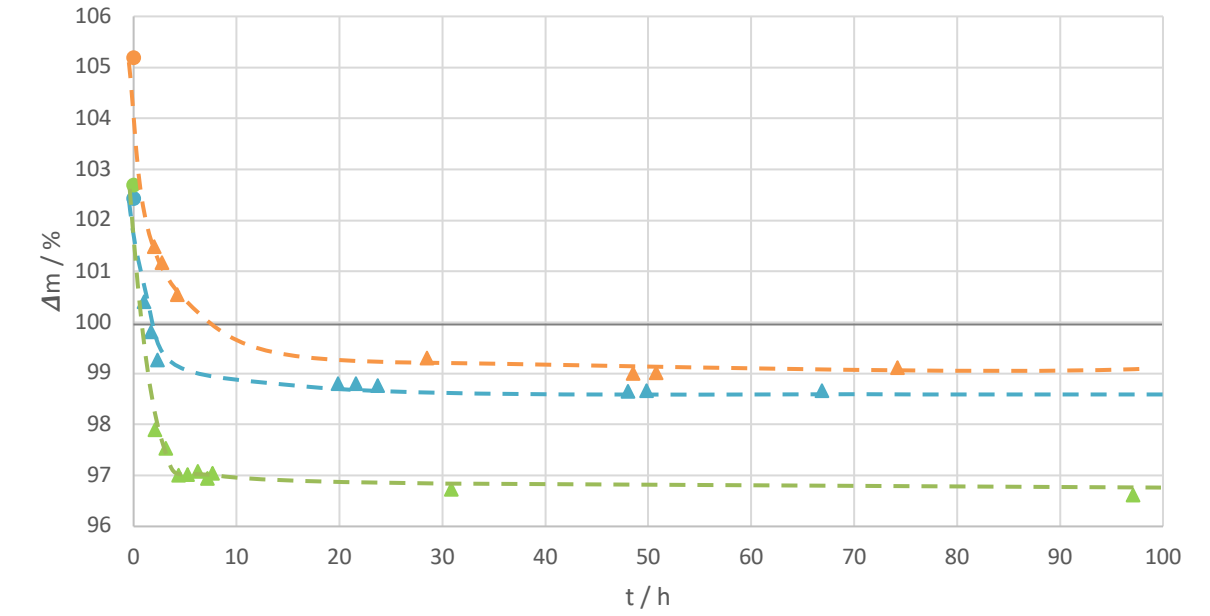

Figure 38: Water content "dried" measurement of cellulose (orange), fine paper (blue) and Kraft sack paper (green) : relative mass change Δm in dependence of time *t* at a temperature of 20°C and a relative humidity of approximately 80 % (blue shaded, dot-markers correspond to wet measurement), 10 % (orange shaded, triangle-markers correspond to dried measurement) and 50 % (diamond-marker correspond to dry measurement). (Lines are drawn for guiding the eyes).

4.4.2 CONTACT ANGLE MEASUREMENT

As shown in the figures in sections 4.1.2, 4.2.2 and 4.3.2, the contact angle measurements for cellulose and fine paper are not easy to perform and the results strongly depend on the time because the droplets disappear in a few seconds and result in a swelling of the paper. Anyhow, it can be concluded that both, cellulose and fine paper, are hydrophilic due to a contact angle smaller than 90°. In the case of cellulose, where the droplet disappears immediately when contacting the surface, one can even speak of superhydrophilicity. On the other hand, Kraft sack paper features a contact angle higher than 90°, which suggests a hydrophobic behaviour. Table 7 summarises these results.

Table 7: Wettability of the investigated materials

Material	Contact angle	Wettability
Cellulose	~ 0°	(super-)hydrophilic
Fine paper	< 90°	hydrophilic
Kraft sack paper	> 90°	hydrophobic

SUMMARY

5 SUMMARY

The last chapter of this thesis gives an overview of the most important findings of the experiments on the three investigated cellulose materials during moisture intake and drying. Additionally, a comparison of the findings and actual scientific literature on moistening and drying processes in cellulose as well as a future outlook of further possible experiments are presented. For reasons of comparison an overview of the most important findings of all measurements carried out are listed in table 8.

Table 8: Summary of the most important results

	cellulose	fine paper	Kraft sack paper
	pure cellulose	cellulose + hemicellulose	cellulose + hemicellulose + lignin
change in mean positron lifetime after moistening $\Delta\tau_{mean,moist}$*	42 ps	20 ps	30 ps
change in mean positron lifetime after drying $\Delta\tau_{mean,dried}$ *	-4 ps	-2 ps	-2 ps
plateaus in mean positron lifetime $\Delta\tau_{mean}$ plotted over time	2	1	2
max. water uptake after moistening Δm_{moist}**	5 %	2 %	3 %
max. water loss after drying Δm_{dried}**	-1 %	-1 %	- 3 %
water absorption time (moistening)	5 h	4 h	4 h
contact angle	< 10°	< 45°	> 90°
wettability	super-hydrophilic	hydrophilic	hydrophobic

*compare to mean positron lifetime at "dry" conditions $\tau_{mean,dry}$
**relative comparison to mass at "dry" conditions m_{dry}

5.1 CELLULOSE

Pure cellulose shows the highest **change in mean positron lifetime** $\Delta\tau_{mean}$ during moistening of all materials investigated of about 42 ps, starting from a mean positron lifetime τ_{mean} in the dry state (laboratory conditions) of $\tau_{mean,dry}$ = 527 ps. The plot of the change in mean positron lifetime $\Delta\tau_{mean}$ in dependence of time (see figure 18) shows two significant increases: the first one starts right away when the sample is placed in humid atmosphere and lasts about 20 hours and raises the mean positron lifetime about 30 ps, the second one after 70 hours of moistening, where the mean positron lifetime changes again about 10 ps. This suggests that there are two different mechanisms of water intake from the surface into the pores of the cellulose on different time scales. After drying the cellulose sample with silica gel, the mean positron lifetime τ_{mean} decreases again, and reaches a value $\tau_{mean,dried}$, which is even slightly lower than the value of the initial dry state. The drying process is faster than the increase during moistening: after about 10 hours of drying the mean positron lifetime has already almost the same value as before moistening in the dry state $\tau_{mean,dry}$. In all three investigated samples there was one lifetime component of the positrons which increased with the water content in the samples and decreased during drying. This lifetime component is in the range of 1400 ps to 1700 ps, which corresponds well to the positron lifetime component of pure water. Table 9 summarizes the mean positron lifetimes of the dry, wet and dried state.

Table 9: Summary of the mean positron lifetime of cellulose
τ_{mean}... mean positron lifetime, τ_i... positron lifetime component i, I_i... Intensity of lifetime component i

state	τ_{mean} [ps]	τ_1 [ps]	I_1 [%]	τ_2 [ps]	I_2 [%]	τ_3 [ps]	I_3 [%]
dry	527.4	178.5	23.9	1508.3	18.4	359.0	57.6
after moistening	569.3	217.0	33.1	1728.8	18.0	379.9	48.9
after drying	523.8	191.7	30.9	1466.0	18.4	38.3	50.7

As well as the change in mean positron lifetime, also **the change in water content** is higher for cellulose compared to fine paper and Kraft sack paper. The mass of the cellulose sample increases more than 5 % when placing it in a surrounding of 80 % relative humidity. The moisture according to the increase of weight Δm uptake takes about 5 hours after the weight of the sample is more or less constant, which means that there is no water uptake anymore. When drying the sample, the mass decreases rapidly, within 3 hours it is the same weight as before moistening and it decreases even further to 99 % of the origin weight, which means that it includes even less water than the sample before moistening. This explains why the mean positron lifetime $\tau_{mean,dried}$ after drying is even slightly lower than before moistening $\tau_{mean,dry}$.

The **contact angle measurements** showed that cellulose is a super-hydrophilic material, which means that all droplets were immediately absorbed from the sample and so the contact angles were significantly lower than 10°.

5.2 FINE PAPER

The **change in mean positron lifetime** $\Delta\tau_{mean}$ for fine paper is the lowest of all investigated materials. The maximum value $\Delta\tau_{mean}$ is about 25 ps, starting from $\tau_{mean,dry}$ = 451 ps in the dry state. After approximately 20 hours this maximum value is reached, there is no second increase like for cellulose and Kraft sack paper. This suggests that the fine paper is more homogenous and the water intake from the surface into the pores takes place within the first 20 hours of moistening. When drying the sample with silica gel the mean positron lifetime τ_{mean} is already after 10 hours as low as it was before moistening. Table 10 summarizes the mean positron lifetimes of the dry, wet and dried state.

Table 10: Summary of the mean positron lifetime of fine paper
τ_{mean}... mean positron lifetime, τ_i... positron lifetime component i, I_i... Intensity of lifetime component i

state	τ_{mean} [ps]	τ_1 [ps]	I_1 [%]	τ_2 [ps]	I_2 [%]	τ_3 [ps]	I_3 [%]
dry	451.2	223.7	39.9	1530.4	11.9	373.6	48.2
after moistening	471.1	252.3	56.6	1639.2	12.3	406.0	31.1
after drying	449.3	236.5	43.5	1461.7	13.0	372.3	43.5

Surprisingly, the **relative mass change due to water uptake** is as low as for Kraft sack paper, although fine paper does not contain hydrophobic lignin. It changes its mass only about 2.5 % when placing it in a wet surrounding. The mass increases within the first five hours and stays more or less constant afterwards. When drying the sample with silica gel, it takes about 2 hours to detract that much water that the sample has the same weight as before moistening.

The **contact angle measurements** showed a hydrophilic behavior. A very accurate measuring of the contact angles was not possible due to the fact that the droplets when placed on the fine paper samples deliquescence within a few seconds.

5.3 KRAFT SACK PAPER

The **change in mean positron lifetime** $\Delta\tau_{mean}$ of the investigated Kraft sack paper samples were about the same amount as for fine paper – the maximum change was a little more than 25 ps, starting from a value in the "dry" state of $\tau_{mean,dry}$ = 475 ps. As well as for pure cellulose, the mean positron lifetime changes in two steps. Also the time of the two increases is very similar as for pure cellulose: from the beginning of moistening the first increase lasts about 20 hours and raises the mean positron lifetime about 20 ps, the second increase is taking place at about 70 hours after placing the sample in a wet surrounding and raises the mean positron lifetime about 5 ps. When drying the sample with silica gel, the mean positron lifetime decreases to the value before moistening, this takes less than 20 hours of drying. Table 11 summarizes the mean positron lifetimes of the dry, wet and dried state of Kraft sack paper.

Table 11: Summary of the mean positron lifetime of Kraft sack paper
τ_{mean}... mean positron lifetime, τ_i... positron lifetime component i, I_i... Intensity of lifetime component i

state	τ_{mean} [ps]	τ_1 [ps]	I_1 [%]	τ_2 [ps]	I_2 [%]	τ_3 [ps]	I_3 [%]
dry	475.1	225.6	39.5	1530.6	12.9	395.2	47.6
after moistening	504.6	233.7	38.3	1688.5	13.6	384.4	48.1
after drying	477.4	23.0	39.9	1514.5	13.0	392.3	47.0

The detection of the **water content** showed that the mass of the sample increases about 2.5 % during moistening, this process seems to be finished after five hours, afterwards the water content stays more or less constant. When placing silica gel in the sample chamber it takes about two hours to dry the sample again.

The **contact angle measurements** showed that Kraft sack paper is hydrophobic, that means the contact angle between the sample and the water droplet which was placed on it is larger than 90°. The measurements showed a contact angle of about (106 ± 6)°.

5.4 OUTLOOK

Further investigations on cellulose materials using PALS will be of high interest because the present study left a few questions open, for example the lifetime components still have to be assigned to different annihilation processes (in bulk, in water, p-Ps formation). For this reason, further PALS measurements which could answer some of these questions are listed in the following.

Positron Annihilation Lifetime Spectroscopy measurements with alcohol

The measurements could be repeated with another liquid, for example alcohol. The different molecule structure and size compared to water could give more insights into the water ad- and absorption processes of cellulose materials. For this purpose, alcohol of high purity would be desired. Due to the in general hygroscopic behaviour of alcohol, which makes it hard to keep the alcohol pure when placed in an environment with air humidity, the simplest secondary alcohol, isopropanol, is a good option. Isopropanol is an isomer of ethylmethylether and the simple alcohol 1-propanol, with long hydrophobic chemical moiety causing why the water intake compared with other alcohols, to be very low.

Positron Annihilation Lifetime Spectroscopy measurements of liquids

If it would be possible to develop an experimental set-up for measuring liquids with PALS, it could be helpful to explain the change of the lifetime components when measuring cellulose materials during the intake of these liquids. Here a big disadvantage of PALS is, that it is not well suited for liquids. If liquids should be investigated with positrons there are two possible experimental set-ups:

1. The ^{22}Na is directly dissolved in the liquid which leads to a radioactive contamination of the liquid sample. The dissolved isotope also influences the annihilation chemically. Many solutes are known to inhibit or quench positronium in water already in small concentrations. Thus, the dissolved radio isotope could lead to wrong interpretations of the measured positron spectrum. Furthermore, positron annihilation with the container wall cannot be avoided.

2. It is very difficult to prepare sources which are waterproof. Usually thin Kapton foils are used, which have to be kept together with special glues because for technical reasons they cannot be weld together. The utilized glues will lead to an additional source component in the positron lifetime spectrum and complicate the analysis of the results.

Positron Annihilation Lifetime Spectroscopy measurements on a longer time scale

The PALS measurements in the "wet" surrounding was carried out for about four days. Figure 35 indicates that there could be a possible third increase in the mean positron lifetime between 90 hours and 100 hours for cellulose and Kraft sack paper. Maybe another, even longer, measurement of cellulose and Kraft sack paper during moisture intake using PALS could show another long-term effect in water ab- and adsorption on different surfaces in these materials.

To obtain a more comprehensive analysis of moisture intake in cellulose materials also other chemical and physical investigations are necessary. Especially where and how the water molecules are bound in the cellulose materials and on which time scale the water is redistributed in the material would be of high interest. Here, PALS measurements without results from a second method for comparison are always very difficult to interpret, but the present thesis shows that it is a reasonable complimentary method for the investigation of cellulose materials, especially for observing long-term processes.

REFERENCES

[1] PARK, Sunkyu; VENDITTI, Richard A.; JAMEEL, Hasan; PAWLAK, Joel J.: Changes in pore size distribution during the drying of cellulose fibers as measured by differential scanning caliometry. Carbohydrate Polymers Volume 66/1 (2006) 97-103

[2] CAO, H.; YUAN, J.-P.; JEAN, Y.C.; PEKAROVICOVA, A.; VENDITTI, R.A.: Subnanometer Hole Properties of Cellulose studied by Positron Annihilaton Lifetime Spectroscopy. American Chemical Society, Structure and Properties of Glassy Polymers (1998) DOI: 10.1021/bk-1998-0710.ch024

[3] OLSSON, Anne-Mari; SALMÉN, Lennart: The association of water to cellulose and hemicellulose in paper examined by FTIR spectroscopy. Carbohydr. Research 339/4 (2003) DOI: 10.1016/j.carres.2004.01.005

[4] GIDLEY, David W.; PENG, Hua-Gen; VALLERY, Richard S.: Positron annihilation as a method to characterize porous materials. Annual Reviews of Materials Research Volume 36 (2006) 49-79

[5] DOYLE, Stephen; MALHORTA, Bansi D.; PEACOCK, Norman; PETHRICK, Richard A.: Positron annihilation and X-ray diffraction Studies of Cellulose and some Derivatives. British Polymer Journal (1984) DOI: https://doi.org/10.1002/pi.4980160105

[6] WEINBERG, Steven: The Quantum Theory of Fields, Volume III, Supersymmetry. New York: Cambridge University Press (1995)

[7] CZICHOS, Horst: Die Welt ist dreieckig – Die Triade Philosophie, Physik und Technik. Springer Verlag, Wiesbaden (2013)

[8] SCHRADER, D.M.; JEAN, Y.C.: Positron and Positronium Chemistry. University of Missouri-Kansas City (1988)

[9] DIRAC, P.A.M.: The quantum theory of the electron. Proceedings of the Royal Society of London Nr. 778 (1928)
URL: http://rspa.Royalsocietypublishing.org/content/royprsa/117/778/610.full.pdf

[10] ANDERSON, Carl D.: The apparent existence of easily deflectable positives. Science 76 Nr. 1967 (1932) 238
URL: http://dx.doi.org/10.1126/science.76.1967.238.

[11] NOBEL MEDIA AB.: The Nobel Foundation. The Nobel Prize in Physics 1959 (2020)
URL: https://www.nobelprize.org/prizes/physics/1959/summary/

[12] KHRAPAK, Alexei G.: Positron and Positronium Annihilation in Gases and Liquids. Linking the Gaseous and Condensed Phases of Matter Volume 326 (1994)

[13] PIRENNE, J.: Ph.D. Thesis. University of Paris. (1944) Arch. Sci Phys.Nat.28 (1946) 233

[14] WHEELER John Achibald: Polyelectrons. Annals of the New York Academic of Science 49 (1946) 219

[15] RICH Arthur: Recent ecperimental advances in positronium research. Reviews of Modern Physics 53 (1981) 127

[16] CIEMAT /GALAN M.: Table de Radionucléides (2009)

[17] HAUTOJÄRVI, P.: Topics in Current Physics: Positrons in Solids. Springer Verlag, Wiesbaden (1979)

[18] PERKINS A.; CARBOTTE J.P.:Effect of the Positron-Phonon Interaction on Positron Motion. Physcial Reviews B 1 (1970) 101, DOI 10.1103/PhysRevB.1.101

[19] WEST R.: Positron studies of condensed matter. Adv. Phys. 22 (1973) 263, DOI 10.1080/00018737300101299

[20] KLINSER, Gregor: Operando Studies of Charging Processes in Battery Cathodes by Magnetometry and Positron Annihilation. Ph.D. Thesis. Technische Universität Graz (2019)

[21] HODGES, C: Trapping of Positrons at Vacancies in Metals. Physical Review Letters 25 (1970) 284

[22] KRAUSE-REHBERG, Reinhard; LEIPNER, Hartmut S.: Positron Annihilation in Semiconductors. Springer-Verlag, Wiesbaden (1999).

[23] COLEMAN, Paul: Positron Beams and Their Applications. World Scientific (2000)

[24] FERRAGUT, R.; CALLONI, A.; DUBASQUIER, A.; CONSOLATI, G.; QUASSO, F.; GIAMMARCHI, M.G.; TREZZI, D.; EGGER, W.; RAVELLI, L.; PETKOV, M.P.; JONES, S.M.; WANG, B.; YAGHI, O.M.; JASINSKA, B.; CHIODINI, N.; PALEARI, A: Positronium formation in porous materials for antihydrogen production. Journal of Physics: Conference Series Volume 225 (2009)

[25] KOTERA, Katsushige; SAITO, Tadashi; YAMANAKA, Taku: Measurement of positron lifetime to probe the mixed molecular states of liquid water. Cornell University. Condesed Matter (2004) DOI 10.1016/j.physleta.2005.07.018

[26] STEPANOV, Sergey V.; BYAKOV, Vsevolod M.; HIRADE, Tetsuya: To the theory of Ps formation. New interpretation of the e+ lifetime spectrum in water. Radiation Physics and Chemistry Volume 76 (2007) 90-95

[27] TUOMISTO, Filip; MAKKONEN, Ilja: Defect identification in semiconductors with positron annihilation: experiment and theory. Reviews of Modern Physics 85 Nr. 4 (2013) 1583

[28] CRAWFORD, R.L.: Lignin biodegradation and transformation. John Wiley and Sons, New York (1981)

[29] PAYEN, Anselme: Mémoire sur la composition du tissu propre des plantes et du ligneux. Comptes rendus Vol. 7 (1838) 1052–1056

[30] YOUNG, Raymond A.; ROWELL, Roger M.: Cellulose structure modification and hydrolysis. Wiley-Interscience, New York (1986) 379

[31] THE EDITORS OF ENCYCLOPAEDOA BRITANNICA: Cellulose. Encyclopædia Britannica inc. (2019) URL: https://www.britannica.com/science/cellulose

[32] COTÉ, Wilfred A.: Chemical Composition of Wood. Springer-Verlag, Berlin (1968)

[33] UPDEGRAFF, D.M.: Semimicro determination of cellulose in biological materials. Analytical Biochemistry 32/3 (1969) 420–424

[34] BROWN R. Malcolm; SAXENA Inder M.: Cellulose: Molecular and Structural Biology. Selected Articles on the Synthesis, Structure, and Applications of Cellulose, Springer Verlag Niederlande (2007)

[35] KRUMM, Christoph; PFAENDTNER, Jim; DAUENHAUER, Paul J.: Millisecond Pulsed Films Unify the Mechanisms of Cellulose Fragmentation. Chemistry of Materials 28/1 (2016) DOI:10.1021/acs.chemmater.6b00580.

[36] CERMAV; CNRS: Structure and morphology of cellulose. CERMAV-CNRS (2009) URL: http://applis.cermav.cnrs.fr/lessons/cellulose/

[37] LECHNER, M.D.; GEHRKE, Klaus; NORDMEIER, Eckhard H.: Makromolekulare Chemie – Ein Lehrbuch für Chemiker, Physiker, Materialwissenschaftler und Verfahrenstechniker. Springer Verlag, Berlin - Heidelberg (2014)

[38] GLAZER, Alexander N.; NIKAIDO, Hiroshi: Microbial Biotechnology. Fundamentals of Applied Microbiology. Second Edition. Freeman, New York (1995)

[39] FRAUNHOFER INFORMATIONSZENTRUM RAUM UND BAU: Organische Dämmstoffe. Fraunhofer IRB (2020)

[40] CHINGA, G.; HELLE, T.; FORSETH, T.: Quantification of structure details of LWC paper coating layers. Nordic Pulp and Paper Research Journal, **17(3)** (2002) 313-318 DOI: 10.3183/NPPRJ-2002-17-03-p313-318

[41] SPRINGER, Roland; RAETHER Friedrich: In situ measurement of light scattering in porous ceramics during sintering. High Temperatures- High Pressures Volume **32** (2000) 385-390, DOI: 10.1068/htwu287

[42] JAYME G.: Mikro-Quellungsmessungen an Zellstoffen, Papier Fabr./Wochbl. Papierfabr. **6** (1944) 187

[43] MINOR, James L.: Hornification – Its Origin and Meaning. Recycling **101** (2010) 93-95

[44] TAO, S.J.: Positronium annihilation in molecular substances. J. Chem. Phys. **56** (1972) 5499 DOI: https://doi.org/10.1063/1.1677067

[45] ELDRUP, M.; LIFHTBODY, D.; SHERWOOD, J.N.: The temperature-depence of positron lifetimes in solid pivalic acid. Chem. Phys. **63** (1981) 51-58 DOI: https://doi.org/10.1016/0301-0104(81)80307-2

[46] CHEMISTRY LIBRETEXTS: Conract angles. Mindtouch (2020) URL: https://chem.libretexts.org/Bookshelves/Physical_and_Theoretical_Chemistry_Textbook_Maps/Supplemental_Modules_(Physical_and_Theoretical_Chemistry)/Physical_Properties_of_Matter/States_of_Matter/Properties_of_Liquids/Contact_Angles

[47] KELLHEIM FIBRES: Funtcional Fibres for nique Products. Kelheim Fibres GmbH (2018) URL: http://www.kelheim-fibres.com/pdf/Functional_Fibres.pdf

[48] MONDI; HENICKL, Petra: Properties Neujet Silk 90 gsm. Acquired at Mondi Uncoated Fine & Kraft Paper GmbH (2018)

[49] FURST, Thomas: Roughness of paper and paperbpard, stylus (Emveco-type) method (Revision of T 575 om-07). Standard Specific Interest Group (2012) URL: https://www.tappi.org/content/tag/sarg/t575.pdf

[50] MONDI: Brown Kraft Sack Paper. Mondi Public limited company (2020) URL:https://www.mondigroup.com/en/products-and-solutions/sack-kraft-paper/sack-kraft-paper-products/advantage-speed/

[51] LEITNER, M.: Synthesis and Positron Annihilation Lifetime Spectroscopy of Nanoporous Platinum. Master Thesis, Technische Universität Graz (2015)

[52] RESCH, Laura; SPRENGEL, Wolfgang; WÜRSCHUM, Roland; SCHENNACH, Robert, KARNER, Anna: Positron Annihilation: A tool for paper Research? Conference proceeding accepted to Progess in Paper Physics Seminar 2020 (2020)

[53] NOROUZI, Hamidreza: Schematich of setup used for static contact angle measurement. Research Gate (2020)
URL: https://www.researchgate.net/figure/Schematic-of-setup-used-for-static-contact-angle-measurement_fig1_323829673

[54] ELDRUP M.; MOGENSEN, O.: Positron lifetime in pure and doped ice and in water. J. Chem. Phys. **57** (1972) 495, DOI: https://doi.org/10.1063/1.1677990

[55] KOTERA, Katsushife; SAITO Tadashi; YAMANAKA, Taku: Measurement of positron lifetime to probe the mixed molecular sattes of liquid water. Physics Letters A **345** (2004) DOI: 10.1016/j.physleta.2005.07.018

APPENDIX

Table 12: PALS measurement of cellulose

t… time, τ_{mean}… mean positron lifetime, $d\tau_{mean}$…uncertainty of the mean positron lifetime, τ_i… positron lifetime component i, $d\tau_i$… uncertainty of the positron lifetime component i (statistic deviation from fitting procedure in PALSfit), I_i… Intensity of lifetime component i

t / h	τ_{mean} / ns	dτ_{mean} / ns	τ_1 / ns	dτ_1 / ns	I_1 /ns	τ_2 / ns	dτ_2 / ns	I_2 / ns	τ_3 / ns	dτ_3 / ns	I_3 / ns
0	0,5274	0,00282	0,17854	0,01626	23,94694	0,35902	0,01542	57,64708	1,5083	0,03068	18,40598
4,75	0,5431	0,0031	0,1972	0,0209	26,172	0,3608	0,0201	55,5239	1,5907	0,0333	18,3041
14,25	0,5592	0,0034	0,1949	0,0238	23,2184	0,3558	0,0189	58,2335	1,654	0,0335	18,5481
23,5	0,559	0,0033	0,1562	0,0183	15,9054	0,3422	0,01	65,2465	1,6496	0,0294	18,8481
32,5	0,5619	0,0037	0,213	0,0191	32,9404	0,3803	0,0256	49,3272	1,7152	0,039	17,7323
41,5	0,5582	0,0034	0,1849	0,0212	21,9129	0,3523	0,0161	59,5315	1,6598	0,0326	18,5556
50,5	0,56	0,0035	0,183	0,0211	21,0409	0,3531	0,0151	60,6581	1,6792	0,0331	18,301
59,5	0,5557	0,0035	0,188	0,019	24,2217	0,3611	0,0167	57,7935	1,6762	0,0348	17,9848
68,5	0,5672	0,0037	0,2107	0,0216	30,1144	0,3714	0,0248	51,5817	1,7147	0,0373	18,1928
77,5	0,5648	0,0038	0,2249	0,0192	37,742	0,3908	0,0325	44,4213	1,7174	0,0411	17,8366
86,5	0,5639	0,0036	0,1736	0,0173	20,7498	0,3572	0,0127	61,2488	1,7171	0,0335	18,0014
95,5	0,5693	0,0037	0,217	0,0204	33,0501	0,3799	0,0271	48,9176	1,7288	0,0383	18,0323
104,75	0,5365	0,003	0,1753	0,0165	22,3881	0,3568	0,0139	59,4658	1,5709	0,0314	18,1461
114,25	0,5266	0,0028	0,1616	0,017	18,9858	0,3472	0,0122	61,842	1,4667	0,0286	19,1722
123,5	0,5322	0,0031	0,1892	0,014	29,2912	0,3848	0,0184	52,8031	1,5281	0,0361	17,9057
132,5	0,533	0,003	0,1903	0,0156	28,2822	0,3771	0,019	53,3552	1,5138	0,0346	18,3626
141,5	0,5205	0,0027	0,1891	0,0212	25,3127	0,3535	0,0213	54,6778	1,396	0,0303	20,0095
150,5	0,5236	0,0028	0,1727	0,0172	22,0096	0,3552	0,015	58,7668	1,4403	0,0299	19,2236
159,5	0,532	0,0031	0,2032	0,0142	34,5083	0,3953	0,0243	47,4175	1,5187	0,0382	18,0742
168,5	0,5238	0,0029	0,2051	0,0163	33,7989	0,3873	0,0267	47,4569	1,4443	0,0366	18,7442
177,5	0,5251	0,0029	0,18	0,0146	26,0651	0,3726	0,0162	55,8187	1,4915	0,0338	18,1162
186,5	0,5184	0,0026	0,15615	0,0161	20,1577	0,349	0,0131	60,0141	1,3939	0,028	19,8282
195,5	0,5238	0,0028	0,1917	0,0138	30,8762	0,3833	0,0201	50,6796	1,466	0,0342	18,4442

Table 13: Water content measurement of cellulose

t… time, Δm… relative mass change

t / h	Δm / %	$\sigma_{\Delta m}$ / %
0,00	100,000	0,013
2,75	103,553	0,014
4,00	104,070	0,014
6,00	105,130	0,014
74,00	105,183	0,014
75,00	105,130	0,014
76,33	105,117	0,014
78,25	105,130	0,014
96,00	105,196	0,014
98,00	101,485	0,013
98,75	101,171	0,013
100,25	100,543	0,013
124,50	99,306	0,013
144,50	99,005	0,013
146,75	99,012	0,013
170,17	99,110	0,013

Table 14: PALS measurement of fine paper

t… time, τ_{mean}… mean positron lifetime, $d\tau_{mean}$…uncertainty of the mean positron lifetime, τ_i… positron lifetime component i, $d\tau_i$… uncertainty of the positron lifetime component i (statistic deviation from fitting procedure in PALSfit), I_i… Intensity of lifetime component i

t / h	τ_{mean} / ns	$d\tau_{mean}$ / ns	τ_1 / ns	$d\tau_1$ / ns	I_1 /ns	τ_2 / ns	$d\tau_2$ / ns	I_2 / ns	τ_3 / ns	$d\tau_3$ / ns	I_3 / ns
0	0,4512	0,0018	0,2237	0,0124	39,909	0,3736	0,0195	48,2127	1,5304	0,0323	11,8783
5	0,4698	0,0034	0,2228	0,0167	41,2255	0,3835	0,0279	47,203	1,7054	0,0559	11,5419
15	0,4735	0,0036	0,2231	0,015	42,4346	0,3915	0,0271	46,1957	1,7412	0,0586	11,3697
25	0,4685	0,003	0,1949	0,0315	20,1195	0,3344	0,0171	67,1117	1,6041	0,0417	12,7688
35	0,469	0,0034	0,2294	0,0186	42,67	0,3829	0,0325	45,6152	1,6769	0,0558	11,7148
45	0,4754	0,0037	0,2465	0,0151	54,597	0,4132	0,0475	33,7726	1,7305	0,0635	11,6304
55	0,467	0,003	0,2055	0,0278	26,4408	0,3433	0,0218	60,6925	1,5877	0,0435	12,8667
65	0,4726	0,0035	0,2358	0,0203	44,6801	0,3826	0,0376	43,5315	1,7026	0,0566	11,7884
75	0,4764	0,0037	0,2343	0,0166	46,2704	0,3948	0,0343	42,3127	1,7597	0,0605	11,4169
85	0,471	0,0035	0,2263	0,0186	41,0978	0,3795	0,0301	47,2578	1,706	0,0559	11,6445
95	0,4677	0,0032	0,2235	0,0248	36,2914	0,36	0,0309	51,3669	1,6339	0,0493	12,3417
105	0,4723	0,0032	0,2139	0,0244	31,5473	0,355	0,0248	55,9308	1,6476	0,0473	12,5219
115	0,4689	0,003	0,1887	0,0283	19,795	0,3333	0,0152	67,4617	1,622	0,0412	12,7433
125	0,476	0,0036	0,2215	0,0183	38,9576	0,3753	0,0266	49,4534	1,7617	0,0552	11,589
135	0,4724	0,0035	0,24	0,0201	47,2859	0,3872	0,0423	40,7659	1,6825	0,0572	11,9482
141,75	0,4711	0,0061	0,2523	0,0328	56,6084	0,406	0,1112	31,0556	1,6392	0,1066	12,336
148,5	0,4558	0,0027	0,2314	0,0447	32,1903	0,3471	0,0446	54,168	1,4167	0,0461	13,6418
158,5	0,4524	0,003	0,2237	0,0197	39,2251	0,3811	0,0311	49,1184	1,5223	0,057	11,6565
168,5	0,4535	0,0029	0,2458	0,021	50,6244	0,398	0,0564	36,8939	1,4594	0,06	12,4817
178,5	0,4515	0,0027	0,2241	0,0337	32,732	0,3526	0,0368	53,8469	1,4025	0,0465	13,4211
188,5	0,4537	0,003	0,2489	0,019	53,4969	0,4083	0,0594	34,313	1,4803	0,0634	12,1901
198,5	0,4527	0,0031	0,2423	0,0186	49,698	0,403	0,0484	38,4803	1,4989	0,0632	11,8217
208,5	0,4566	0,003	0,2385	0,0195	46,9156	0,3964	0,0444	40,9375	1,502	0,0594	12,1469
216	0,4493	0,0039	0,2365	0,0375	43,5144	0,3723	0,0691	43,4561	1,4167	0,074	13,0295

Table 15: Water content measurement of fine paper

t… time, Δm… relative mass change

t / h	Δm / %	$\sigma_{\Delta m}$ / %
0,00	100,000	0,011
1,00	101,346	0,012
1,92	101,903	0,012
3,00	102,181	0,012
4,27	102,289	0,012
5,00	102,300	0,012
6,23	102,346	0,012
26,92	102,465	0,012
27,83	102,425	0,012
49,45	102,403	0,012
52,42	102,369	0,012
77,42	102,357	0,012
173,50	102,425	0,012
174,50	100,409	0,012
175,17	99,813	0,012
175,80	99,262	0,012
193,33	98,802	0,012
195,10	98,796	0,012
197,22	98,762	0,012
221,50	98,648	0,012
223,33	98,665	0,012
240,33	98,665	0,012

Table 16: PALS measurement of Kraft sack paper

t… time, τ_{mean}… mean positron lifetime, $d\tau_{mean}$…uncertainty of the mean positron lifetime, τ_i… positron lifetime component i, $d\tau_i$… uncertainty of the positron lifetime component i (statistic deviation from fitting procedure in PALSfit), I_i… Intensity of lifetime component i

t / h	τ_{mean} / ns	$d\tau_{mean}$ / ns	τ_1 / ns	$d\tau_1$ / ns	I_1 /ns	τ_2 / ns	$d\tau_2$ / ns	I_2 / ns	τ_3 / ns	$d\tau_3$ / ns	I_3 / ns
0	0,4751	0,0021	0,2256	0,0123	39,4782	0,3952	0,0212	47,5830	1,5306	0,0364	12,9388
5	0,4880	0,0032	0,1930	0,0288	19,3737	0,3495	0,0160	67,2819	1,6143	0,0435	13,3444
15	0,4950	0,0033	0,2325	0,0263	36,2577	0,3763	0,0349	49,8536	1,6064	0,0483	13,8887
25	0,4979	0,0033	0,2053	0,0269	24,0020	0,3567	0,0194	62,3955	1,6620	0,0440	13,6025
35	0,4978	0,0034	0,2254	0,0228	35,6235	0,3759	0,0299	50,7469	1,6638	0,0484	13,6296
45	0,4942	0,0032	0,2059	0,0304	22,5836	0,3526	0,0200	63,6834	1,6250	0,0431	13,7329
55	0,4948	0,0032	0,1982	0,0300	20,2002	0,3490	0,0174	65,9728	1,6242	0,0418	13,8270
65	0,5027	0,0034	0,2091	0,0308	23,5563	0,3530	0,0211	62,5558	1,6754	0,0434	13,8879
75	0,4994	0,0031	0,1922	0,0297	18,7341	0,3458	0,0159	66,8884	1,6142	0,0393	14,3775
86,5	0,5046	0,0032	0,2337	0,0208	38,2724	0,3844	0,0307	48,0862	1,6885	0,0457	13,6414
98	0,4852	0,0030	0,1897	0,0247	20,5212	0,3503	0,0155	65,6000	1,5593	0,0402	13,8788
108	0,4759	0,0029	0,2253	0,0200	38,3767	0,3864	0,0326	47,8575	1,4855	0,0490	13,7658
118	0,4772	0,0031	0,2310	0,0181	41,2727	0,4002	0,0355	45,8991	1,5455	0,0548	12,8282
128	0,4729	0,0027	0,1811	0,0203	21,0003	0,3531	0,0141	65,1320	1,4770	0,0394	13,8677
138	0,4742	0,0028	0,2084	0,0258	27,3298	0,3591	0,0235	58,5762	1,4678	0,0423	14,0940
148	0,4717	0,0026	0,2043	0,0310	23,8940	0,3471	0,0233	61,1842	1,4106	0,0385	14,9217
160	0,4774	0,0027	0,2297	0,0171	39,9052	0,3923	0,0291	47,0468	1,5415	0,0459	13,0480

Table 17: Water content measurement of Kraft sack paper

t… time, Δm… relative mass change

t / h	Δm / %	$\sigma_{\Delta m}$ / %
0,00	100,000	0,012
0,67	100,743	0,013
1,67	101,593	0,013
3,50	102,247	0,013
4,67	102,318	0,013
6,33	102,366	0,013
25,33	102,621	0,013
27,08	102,615	0,013
29,33	102,633	0,013
95,00	102,693	0,013
97,08	97,898	0,013
98,08	97,537	0,013
99,33	97,003	0,013
100,25	97,016	0,013
101,22	97,083	0,013
102,17	96,950	0,013
102,68	97,043	0,013
125,83	96,729	0,013
192,08	96,616	0,013